Meteoritics & Planetary Science 37, 91–111 (2002)
Available online at http://www.uark.edu/meteor

Anorthite-rich chondrules in CR and CH carbonaceous chondrites: Genetic link between calcium-aluminum-rich inclusions and ferromagnesian chondrules

ALEXANDER N. KROT* AND KLAUS KEIL

Hawai'i Institute of Geophysics and Planetology, School of Ocean and Earth Science and Technology, University of Hawai'i at Manoa, Honolulu, Hawai'i 96822, USA
*Correspondence author's e-mail address: sasha@higp.hawaii.edu

(Received 2001 May 16; accepted in revised form 2001 October 9)

Abstract–Anorthite-rich chondrules in CR and CH carbonaceous chondrites consist of magnesian low-Ca pyroxene and forsterite phenocrysts, FeNi-metal nodules, interstitial anorthite, Al-Ti-Cr-rich low-Ca and high-Ca pyroxenes, and crystalline mesostasis composed of silica, anorthite and high-Ca pyroxene. Three anorthite-rich chondrules contain relic calcium-aluminum-rich inclusions (CAIs) composed of anorthite, spinel, ±Al-diopside, and ±forsterite. A few chondrules contain regions which are texturally and mineralogically similar to magnesian (type I) chondrules and consist of forsterite, low-Ca pyroxene and abundant FeNi-metal nodules. Anorthite-rich chondrules in CR and CH chondrites are mineralogically similar to those in CV and CO carbonaceous chondrites, but contain no secondary nepheline, sodalite or ferrosilite. Relatively high abundances of moderately-volatile elements such as Cr, Mn and Si in the anorthite-rich chondrules suggest that these chondrules could not have been produced by volatilization of the ferromagnesian chondrule precursors or by melting of the refractory materials only. We infer instead that anorthite-rich chondrules in carbonaceous chondrites formed by melting of the reduced chondrule precursors (olivine, pyroxenes, FeNi-metal) mixed with the refractory materials, including relic CAIs, composed of anorthite, spinel, high-Ca pyroxene and forsterite. The observed mineralogical and textural similarities of the anorthite-rich chondrules in several carbonaceous chondrite groups (CV, CO, CH, CR) may indicate that these chondrules formed in the region(s) intermediate between the regions where CAIs and ferromagnesian chondrules originated. This may explain the relative enrichment of anorthite-rich chondrules in ^{16}O compared to typical ferromagnesian chondrules (Russell *et al.*, 2000).

INTRODUCTION

The short-lived radionuclide ^{26}Al was present in the nebular regions where the first solids in our solar system, calcium-aluminum-rich inclusions (CAIs) and chondrules, formed (Lee *et al.*, 1976; Hutcheon and Hutchison, 1989; Goswami *et al.*, 1994; MacPherson *et al.*, 1995; Russell *et al.*, 1996, 1997a; Srinivasan *et al.*, 1996a,b; Mostefaoui *et al.*, 1999; Goswami and Vanhala, 2000; Kita *et al.*, 2000; McKeegan *et al.*, 2000a; Ito *et al.*, 2000; Yurimoto *et al.*, 2000; Hutcheon *et al.*, 2000). It is commonly believed that chondrules formed 2–5 Ma after CAIs (*e.g.*, Podosek and Cassen, 1994; MacPherson *et al.*, 1995). This hypothesis is based on the assumption that ^{26}Al was initially homogeneously distributed in the nebular regions from which both CAIs and chondrules formed, and the observation that many CAIs from different chondrite groups have the "canonical" $(^{26}Al/^{27}Al)_I$ ratio of about $(4–5) \times 10^{-5}$, whereas chondrules analyzed so far have $(^{26}Al/^{27}Al)_I$ ratios of $<1.5 \times 10^{-5}$ (MacPherson *et al.*, 1995; Russell *et al.*, 1996, 1997a; Mostefaoui *et al.*, 1999; Kita *et al.*, 2000; McKeegan *et al.*, 2000a). Unfortunately, only a few ferromagnesian chondrules contain phases with high enough Al/Mg ratios (>40) for $^{26}Mg^*$ to be detected by secondary ion mass spectrometry, and the ^{26}Al-^{26}Mg isotope systematics have been largely studied for rare Al-rich chondrules.

Based on the correlated occurrences of ^{26}Al and ^{41}Ca in CAIs, Sahijpal *et al.* (1998) concluded that both short-lived radionuclides had a stellar origin and were injected into the protosolar cloud during its collapse. This process would probably result in homogeneous distribution of ^{26}Al in both CAI- and chondrule-forming regions (Sahijpal *et al.*, 1998), although local heterogeneity could be produced as well (Vanhala and Boss, 2000).

Alternatively, it was suggested that CAIs and chondrules formed in separate and isotopically distinct reservoirs and were later mixed in various accretion regions (Shu *et al.*, 1996; Wood, 1996, 1998a,b; McKeegan *et al.*, 1998, 2000a,b; Krot *et al.*, 1999a,b; Guan *et al.*, 2000a,b; Fagan *et al.*, 2000a,b). Although this might weaken the chronological significance of Al-Mg systematics for understanding the time difference

Prelude preprint MS#4553

between CAI and chondrule formation, the Al-Mg systematics remains valid for dating the complex histories of CAIs (MacPherson and Davis, 1993; Hsu *et al.*, 2000).

Aluminum-magnesium isotope measurements of Al-rich chondrules were largely made on meteorites that experienced mild thermal metamorphism (Chainpur, L3.4; Inman, LL3.3/3.6; Bovedy, L3.7; Kainsaz, CO3.1; Ornans, CO3.3) or late-stage alteration (Allende, CV3) (Hutcheon and Hutchison, 1989; Sheng *et al.*, 1991; Hutcheon and Jones, 1995; Russell *et al.*, 1996, 1997a; Srinivasan *et al.*, 1996a; Mostefaoui *et al.*, 1999; Kita *et al.*, 2000; Wadhwa and Russell, 2000). Both processes may have reset or disturbed the ^{26}Al-^{26}Mg systematics in these chondrules (LaTourrette and Wasserburg, 1998; LaTourrette and Hutcheon, 1999; Yurimoto *et al.*, 2000). Systematic Al-Mg isotope studies of chondrules from the most primitive carbonaceous chondrites are virtually non-existent.

Using high-resolution x-ray elemental mapping techniques, we discovered that relatively primitive CR, CH, reduced CV and the unique carbonaceous chondrites Adelaide and Acfer 094 commonly contain (1–10 per thin section) a subset of Al-rich chondrules—anorthite-rich chondrules (ARCs) (Krot *et al.*, 1999b; Krot, 2000; Hutcheon *et al.*, 2000; Marhas *et al.*, 2000). The presence of ARCs in primitive carbonaceous chondrites and their unique mineralogical features (coarse-grained, igneous anorthite and relic CAIs) make them ideal for Al-Mg isotope studies to understand (1) the distribution of ^{26}Al in chondrule-forming regions, (2) the time difference between CAI and chondrule formation, and (3) the genetic relationship between chondrules and CAIs.

Here we present mineralogical and petrographic studies of ARCs in CR and CH carbonaceous chondrites. Magnesium- and oxygen-isotopic studies of these chondrules are in progress and will be reported in a separate paper.

PLAGIOCLASE-OLIVINE INCLUSIONS AND ANORTHITE-RICH CHONDRULES IN CARBONACEOUS CHONDRITES: PREVIOUS STUDIES

Plagioclase-olivine inclusions (POIs) described by Sheng *et al.* (1991) in the CV chondrite Allende consist mainly of plagioclase and olivine and range in composition from type C CAIs to porphyritic olivine chondrules. In contrast to the CAIs, POIs are characterized by the absence of melilite, platinum group element (PGE) nuggets and Wark–Lovering rims, the abundance of olivine, a distinctive pyroxene composition (TiO_2/Al_2O_3 ratio of ~1), and more sodic plagioclase (An_{85-95}). Sheng *et al.* (1991) excluded the possibility of formation of POIs as liquid or solid condensates from a solar gas or as evaporative residues and suggested that POIs formed by aggregation of isotopically dissimilar materials followed by partial melting.

Kring and Holmen (1988) first described a new class of chondrules with refractory inclusion affinities, ARCs, in the CV chondrites Allende, Ningqiang and Kaba and CO chondrite Kainsaz. The ARCs are compositionally intermediate between ferromagnesian chondrules and CAIs, and are mineralogically different from most of the Ca, Al-rich chondrules described by Bischoff and Keil (1984), Bischoff *et al.* (1985) and Huss *et al.* (2001) in ordinary chondrites. ARCs can be considered as a subset of Ca, Al-rich chondrules as defined by Bischoff and Keil (1984). These chondrules have a droplet morphology and igneous textures and consist of abundant anorthitic plagioclase, ±spinel, ±olivine, ±pigeonite, ±enstatite, ±augite, ±fassaite, and always contain small amounts of Fe-metal/sulfides. POIs as defined by Sheng *et al.* (1991) are a subset of ARCs (Kring and Holmen, 1988). The ARCs are enriched in moderately volatile lithophile elements; their element abundances increase almost monotonically with volatility. The rare earth elements (REE) in most of the ARCs are unfractionated, similar to those in ferromagnesian chondrules. Some of the ARCs have highly fractionated REE patterns, similar to volatility-controlled group II and ultrarefractory patterns seen in refractory inclusions (Kring and Boynton, 1990). The oxygen-isotopic compositions of two ARCs analyzed are similar to the most ^{16}O-rich porphyritic chondrules in Allende (Kring and Holmen, 1988). Kring and Boynton (1990) concluded that some of the precursors of ARCs and refractory inclusions may have come from the same reservoir, or from different and isolated reservoirs in which similar processes operated.

MacPherson and Russell (1997) discussed several possible models for the origin of Al-rich chondrules including impact melting, precursor mixing, and volatilization and concluded that no single model appears capable of explaining the entire spectrum of Al-rich chondrule bulk compositions.

Studies of Ca, Al-rich chondrules and/or anorthite-rich chondrules in CR chondrites are very limited (Weber and Bischoff, 1997; Weisberg *et al.*, 2001). Weber and Bischoff (1997) found two ARCs composed of elongated forsteritic olivines surrounded by laths of fassaite and anorthite and having igneous, barred olivine textures in the Acfer 059-El Djouf 001 chondrite (one of these chondrules is described by Bischoff *et al.*, 1993). Weisberg *et al.* (2001) described one spherical ARC (~900 μm in diameter) in the Renazzo chondrite. It consists (in vol%) of anorthitic plagioclase (An_{98}) (55%), Al-Ti-bearing low-Ca pyroxene (26%) and high-Ca pyroxene (14%), forsterite (2%), and Cr-Ti-bearing spinel (2%). Anorthite has an essentially flat, group I REE pattern at ~20 × CI and contains isotopically normal Mg (initial ^{26}Al/^{27}Al < 1.8 × 10^{-5}).

ANALYTICAL PROCEDURES

Twenty one polished thin sections of the CR chondrites Acfer 139, Acfer 087, El Djouf 001, Al Rais, Elephant Moraine (EET) 87730, EET 87770, EET 92042, EET 92174, Graves Nunataks (GRA) 95229, MacAlpine Hills (MAC) 87320, and Pecora Escarpment (PCA) 91082 and 12 polished thin sections

TABLE 1. List of polished thin sections of CR and CH chondrites studied.

Chondrite	pts	chd no.	Chondrite	pts	chd no.
CR chondrites					
Acfer 087	AB	8	GRA 95229	18	7
Acfer 139	AG	7	GRA 95229	21	10
EET 87730	30	2	GRA 95229	29	3
EET 87747	17	8	MAC 87320	9	1
EET 87770	14	6	MAC 87320	11	5
EET 92041	21	4	MAC 87320	20	5
EET 92042	23	2	PCA 91082	6	4
EET 92042	22	3	PCA 91082	20	6
EET 92147	7	1	PCA 91082	26	2
El Djouf 001	AB	4	PCA 91082	28	6
CH chondrites					
Acfer 182	AB1	1	ALH 85085	8	0
Acfer 182	AB2	0	PCA 91452	6	0
Acfer 182	AB3	0	PCA 91467	21	0
Acfer 182	AMNH-2	0	PAT 91546	22	0
Acfer 182	AMNH-5	0	PAT 91546	23	0
Acfer 207	AMNH-4	0	RKP 92435	10	0

pts = polished thin section; chd no. = number of anorthite-rich chondrules identified.
Abbreviations in pts (polished thin sections) column are as follows: AB = Addi Bischoff; AG = Ansgar Greshake; AMNH = American Museum of Natural History; number = Antarctic Meteorite Working Group designations.

of the CH chondrites Acfer 182, Acfer 207, Allan Hills (ALH) 85085, Patuxent Range (PAT) 91546, PCA 91328, PCA 91452, PCA 91467 and Reckling Peak (RKP) 92435 (Table 1) were studied using optical microscopy, backscattered electron (BSE) imaging, x-ray elemental mapping, and quantitative electron probe microanalysis (EPMA). To identify Al-rich objects (CAIs and Al-rich chondrules) in the CR and CH chondrites, x-ray elemental maps with resolutions of 2–5 μm/pixel were acquired using five spectrometers of a Cameca SX-50 microprobe at 15 kV accelerating voltage, 50–100 nA beam current and ~1–2 μm beam size. The elemental maps in Mg, Ca, and Al Kα were combined using a RGB color scheme and ENVI software. BSE images were obtained with a Zeiss DSM-962 scanning electron microscope (SEM) using a 15 kV accelerating voltage and 1–2 nA beam current. Electron probe microanalyses were performed with the Cameca SX-50 microprobe using a 15 kV accelerating voltage, 10–20 nA beam current, beam size of ~1–2 μm and wavelength dispersive x-ray spectroscopy. For each element, counting times on both peak and background were 30 s (10 s for Na and K). Matrix effects were corrected using PAP procedures. The element detection limits with the Cameca SX-50 are (in wt%): SiO_2, Al_2O_3, MgO, 0.03; TiO_2, CaO, K_2O, 0.04; Na_2O, Cr_2O_3, 0.06; MnO, 0.07; FeO, 0.08.

RESULTS

Anorthite-rich chondrules are rare, but ubiquitous (~5 per thin section) in nearly all CR chondrites studied (no ARCs were found in Al Rais); ARCs are virtually absent in CH chondrites (Table 1). The only ARC found in CH chondrites (Acfer 182), however, contains a relic CAI, and will be described in a separate section below.

Anorthite-Rich Chondrules in CR Chondrites

ARCs in CR chondrites have porphyritic or microporphyritic textures and are magnesium-rich (Fa and Fs contents of olivine and pyroxenes <2–3 mol%). They consist of low-Ca pyroxene and olivine phenocrysts, interstitial plagioclase, low-Ca and high-Ca pyroxenes, FeNi-metal nodules, and crystalline mesostasis; spinel is generally minor (Figs. 1–4). Based on the modal abundances of olivine and low-Ca pyroxene, ARCs can be divided into olivine-rich and pyroxene-rich varieties (Figs. 1 and 2). Although there is a continuum between these chondrule types, the pyroxene-rich ARCs are much more abundant than the olivine-rich ARCs. One of the ARCs is dominated by anorthite and high-Ca pyroxene (Fig. 4). Two anorthite-rich chondrules in EET 92147 (Fig. 3) and Acfer 087 (Fig. 5) contain inclusions of CAI-like objects.

Low-Ca pyroxene occurs as coarse-grained subhedral phenocrysts, typically occupying chondrule peripheries (Fig. 1a,d) and as elongated grains overgrown by high-Ca pyroxene in the interstitial regions (Figs. 1c and 2c,f). The low-Ca pyroxene phenocrysts are either enstatite ($Fs_{0.5-1}Wo_{1-5}$) or pigeonite ($Fa_{1-2}Wo_{5-8}$) in composition; the interstitial low-Ca

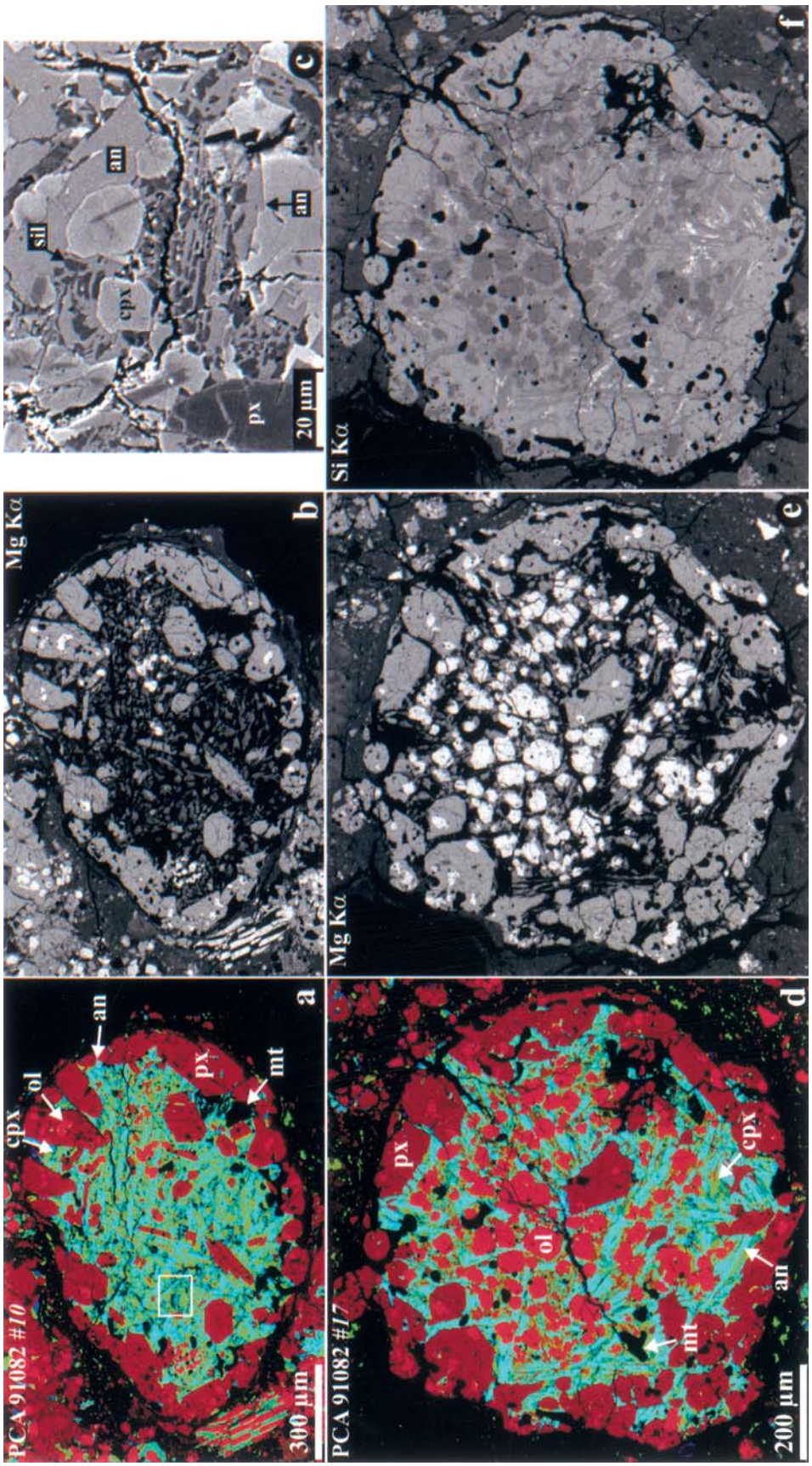

FIG. 1. Combined x-ray elemental maps in Mg (red), Ca (green) and Al Kα (blue) (a, d), elemental maps in Mg (b, e) and Si Kα (f) x-rays and backscattered electron image (c) of the anorthite-rich chondrules #10 (a–c) and #17 (d–f) in the CR chondrite PCA 91082. The chondrules consist of low-Ca pyroxene (px), forsterite (ol), anorthite (an), high-Ca pyroxene (cpx), FeNi-metal nodules (mt) and silica-rich crystalline mesostasis composed of anorthite, silica (sil) and high-Ca pyroxene. Low-Ca pyroxene occurs as elongated grains overgrown by high-Ca pyroxene in the chondrule cores and as phenocrysts poikilitically enclosing forsterite grains in chondrule peripheries. Region outlined in (a) is shown in (c).

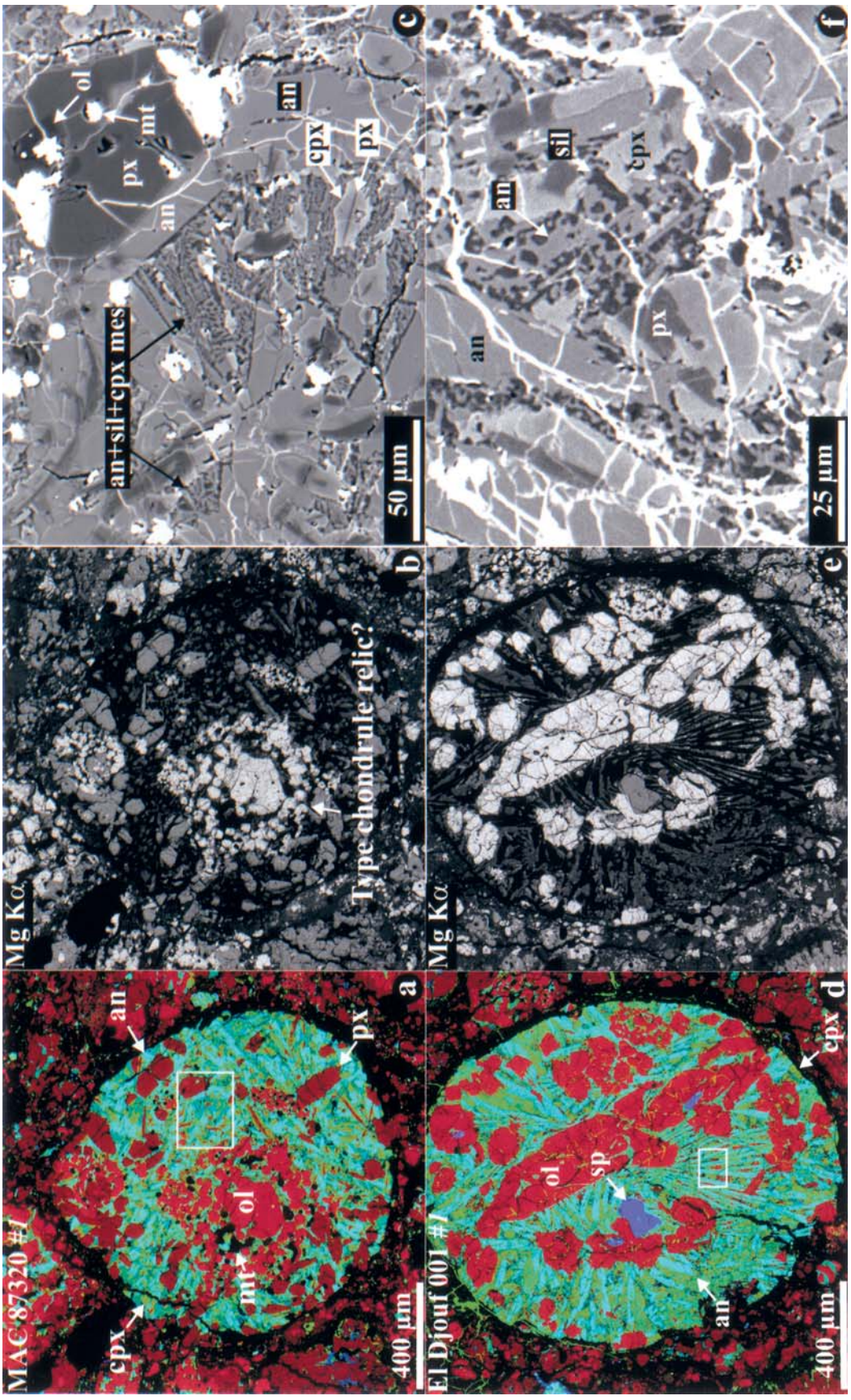

FIG. 2. Combined x-ray elemental maps in Mg (red), Ca (green) and Al Kα (blue) (a, d), elemental maps in Mg (b, e) and backscattered electron images (c, f) of the anorthite-rich chondrules #1 in the CR chondrites MAC 87320 (a–c) and El Djouf 001 (d–f). (a–c) Chondrule consists of low-Ca pyroxene (px), forsterite (ol), anorthite (an), high-Ca pyroxene (cpx), FeNi-metal nodules (mt) and silica-rich crystalline mesostasis composed of anorthite, silica (sil) and high-Ca pyroxene. Low-Ca pyroxene occurs as elongated grains overgrown by high-Ca pyroxene and as phenocrysts surrounded by anorthite or by mesostasis. Forsterite grains are concentrated in several regions containing abundant FeNi-metal nodules. (d–f) Chondrule consists of forsterite, spinel (sp), anorthite, low-Ca and high-Ca pyroxenes, and silica-rich crystalline mesostasis composed of anorthite, silica (sil) and high-Ca pyroxene. Low-Ca pyroxene occurs as elongated grains overgrown by high-Ca pyroxene. Regions outlined in (a) and (d) are shown in (c) and (f), respectively. White vein-like features in (c) and (f) are cracks filled by terrestrial weathering products.

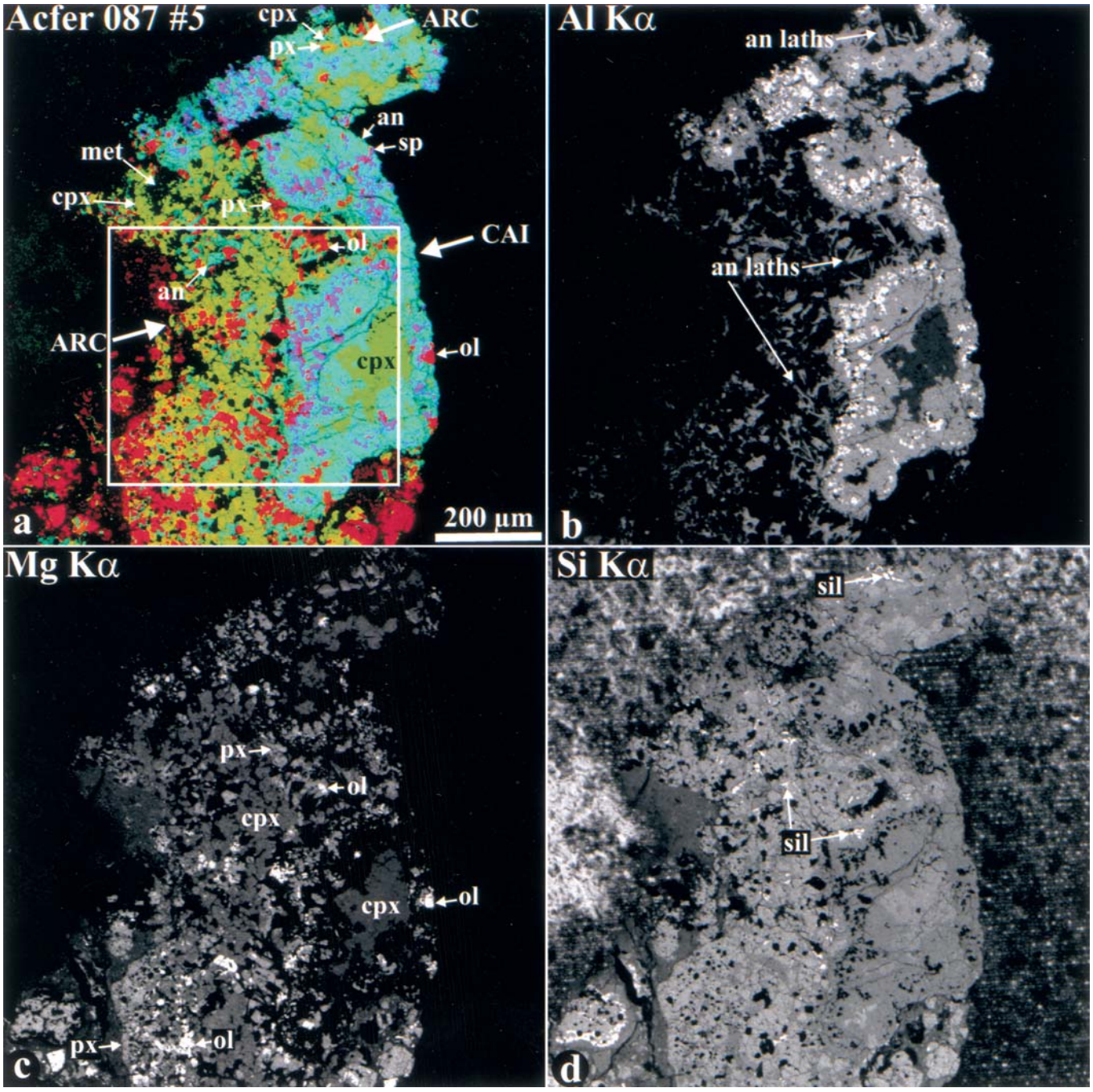

FIG. 3. *(above and on facing page)* Combined x-ray elemental map in Mg (red), Ca (green) and Al Kα (blue) (a), elemental map in Mg Kα (b) and backscattered electron images (c–f) of anorthite-rich chondrule #1 containing relic CAI-like object in the CR chondrite Acfer 187. The chondrule consists of low-Ca pyroxene and forsterite phenocrysts, high-Ca pyroxene, anorthite, abundant FeNi-metal nodules and silica-anorthite-high-Ca pyroxene mesostasis (mes). The CAI-like object consists of spinel, forsterite, and anorthite; it is metal-free. Regions outlined in (a) are shown in detail in (d), (e) and (f).

pyroxenes are pigeonites. Both textural types of pyroxenes have high contents of Al_2O_3 (0.5–4 wt%), TiO_2 (up to 1.2 wt%) and Cr_2O_3 (0.4–1.6 wt%) and moderate concentrations of MnO (0.1–0.6 wt%) (Table 2; Figs. 6 and 7).

High-Ca pyroxenes ($Fs_{1-2}Wo_{35-45}$) occurring in the interstitial regions and chondrule mesostases have higher concentrations of Al_2O_3 (1–6 wt%), TiO_2 (0.5–5.5 wt%), Cr_2O_3 (0.3–3 wt%) and MnO (up to 2.5 wt%) than the low-Ca pyroxenes; the highest concentrations of these elements are found in pyroxenes in mesostases (Table 2; Fig. 7).

Olivine occurs as poikilitic inclusions in low-Ca pyroxene phenocrysts (Fig. 1a,d) and as subhedral-to-euhedral

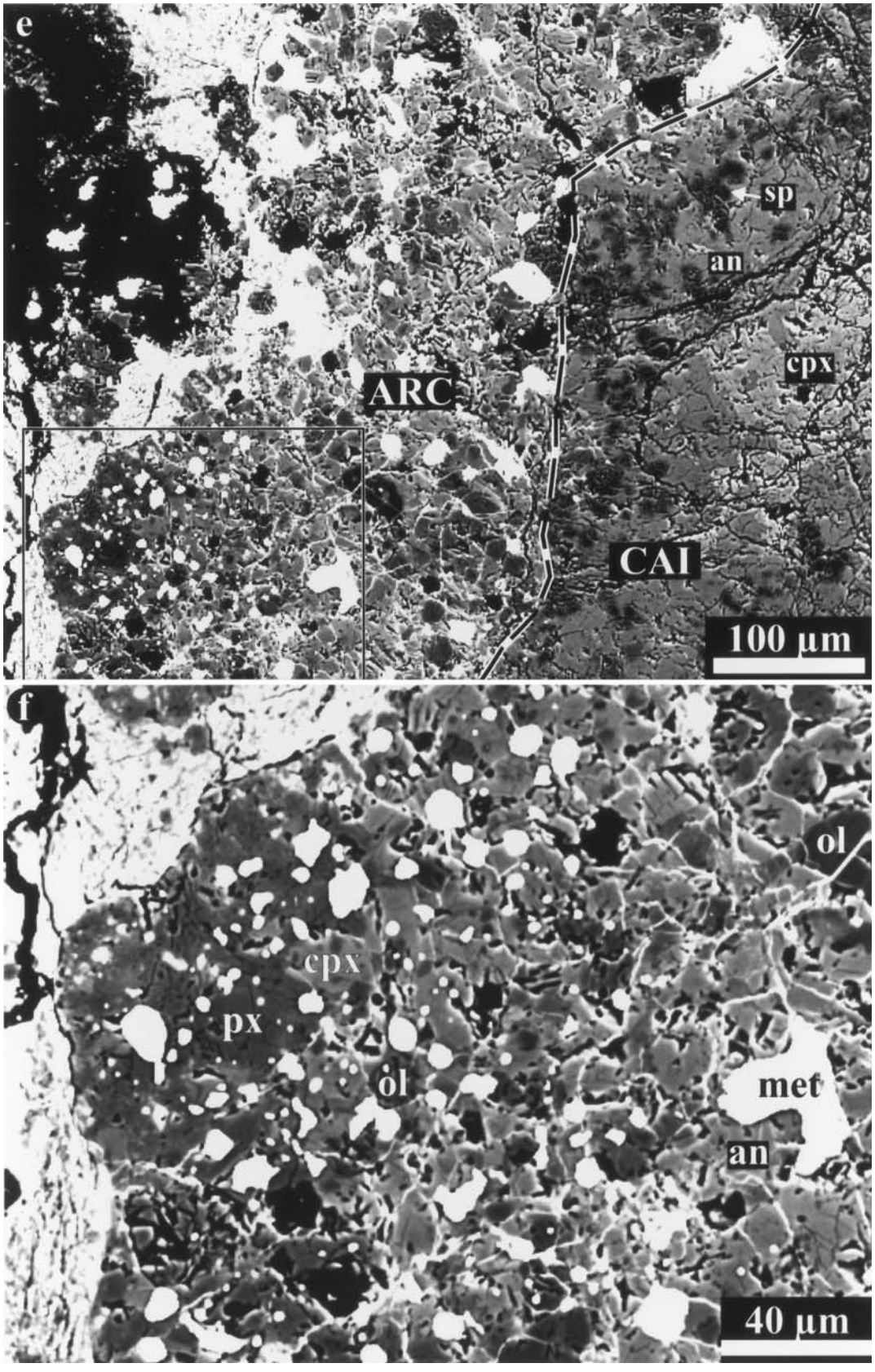
e
sp
an
cpx
ARC
CAI
100 µm
f
ol
cpx
px
ol
met
an
40 µm

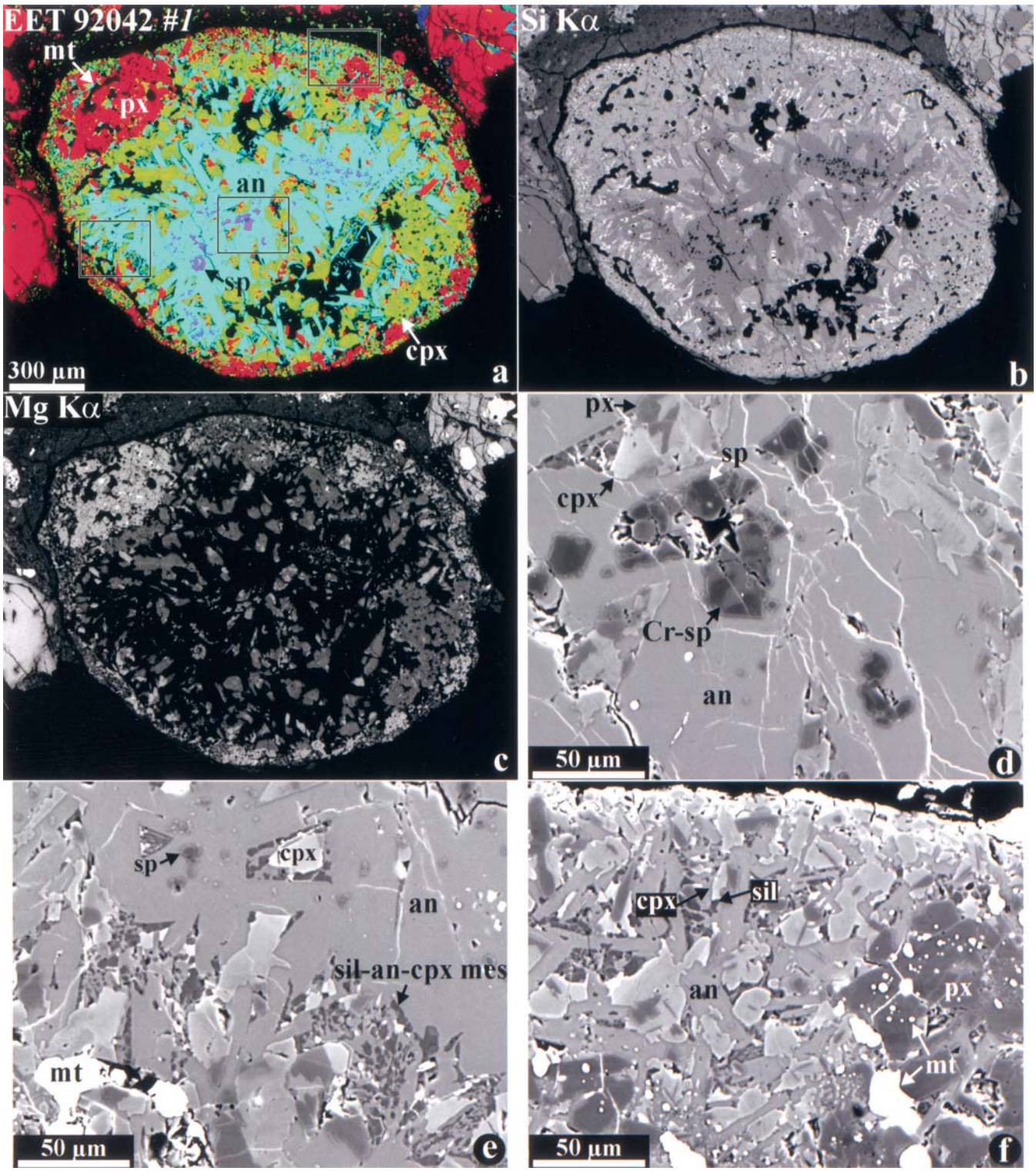

FIG. 4. Combined x-ray elemental map in Mg (red), Ca (green) and Al Kα (blue) (a), elemental maps in Si (b) and Mg Kα (c) and backscattered electron images (d–f) of the anorthite-rich chondrule #1 in the CR chondrite EET 92042. The chondrule consists of anorthite poikilitically enclosing Cr-rich (Cr-sp) and Cr-poor (sp) spinel grains, high-Ca pyroxene, low-Ca pyroxene, FeNi-metal nodules, minor forsterite and silica-rich crystalline mesostasis composed of silica, anorthite and high-Ca pyroxene. Regions outlined in (a) are shown in detail in (d), (e), and (f).

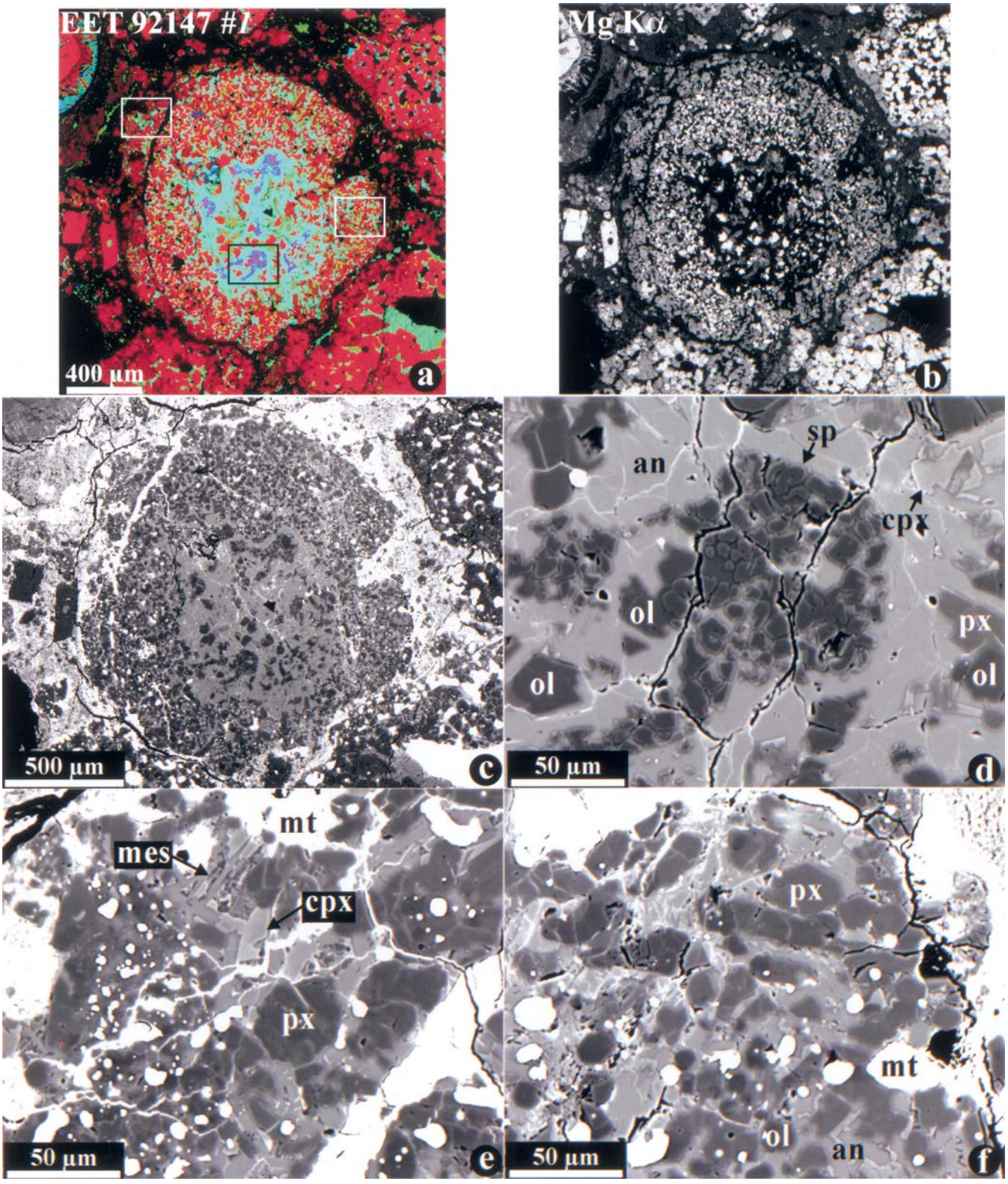

FIG. 5. Combined x-ray elemental map in Mg (red), Ca (green) and Al Kα (blue) (a), elemental maps in Al (b), Mg (c) and Si Kα (d) and backscattered electron images (e, f) of the anorthite-rich chondrule #5 associated with CAI in the CR chondrite Acfer 187. The chondrule consists of high-Ca pyroxene, low-Ca pyroxene, forsterite, lath-shaped anorthite, silica-bearing mesostasis and abundant FeNi-metal nodules. The CAI consists of diopside (cpx), anorthite, spinel and minor forsterite; it is metal-free. Regions outlined in (a) and (e) are shown in detail in (e) and (f), respectively.

TABLE 2. Representative microprobe analyses of pyroxenes in ARCs in CR and CH chondrites.

an.	1	2	3	4	5	6	7	8	9
min	en	en	pig	pig	aug	aug	aug	aug	aug
SiO_2	58.6	58.5	57.4	57.5	53.6	53.5	52.1	48.9	49.1
TiO_2	0.10	0.33	0.54	0.47	1.1	1.4	2.3	4.7	5.2
Al_2O_3	1.1	1.3	1.3	2.2	2.2	2.9	3.0	5.5	5.2
Cr_2O_3	0.67	0.54	1.0	0.81	1.5	0.67	1.4	2.7	1.9
FeO	0.85	0.46	1.6	0.72	1.1	0.45	1.1	1.1	0.64
MnO	<0.07	<0.07	0.29	0.16	0.43	0.22	0.56	0.66	0.34
MgO	38.5	38.5	35.5	34.8	22.4	20.6	20.0	17.5	17.1
CaO	0.45	0.55	2.7	4.4	17.2	20.5	18.9	19.1	20.5
Na_2O	<0.06	<0.06	<0.06	<0.06	<0.06	<0.06	<0.06	<0.06	<0.06
K_2O	<0.04	<0.04	<0.04	<0.04	<0.04	<0.04	<0.04	<0.04	<0.04
Total	100.2	100.3	100.3	101.1	99.5	100.2	99.4	100.1	100.1
Fs	1.2	0.7	2.3	1.1	1.7	0.7	1.8	1.9	1.1
Wo	0.8	1.0	5.1	8.3	35.0	41.4	39.7	43.1	45.7

an. = analysis number; an. 1, 5, 8 = PCA 91082, 16 (chd #17); an. 2, 4, 9 = MAC 87320, 9 (chd #1); an. 3, 7 = Acfer 182, AB (chd #1); an. 1, 2 = phenocrysts; an. 3–6 = interstitial regions; an. 7, 8 = mesostasis; en = low-Ca pyroxene; pig = pigeonite; aug = augite.

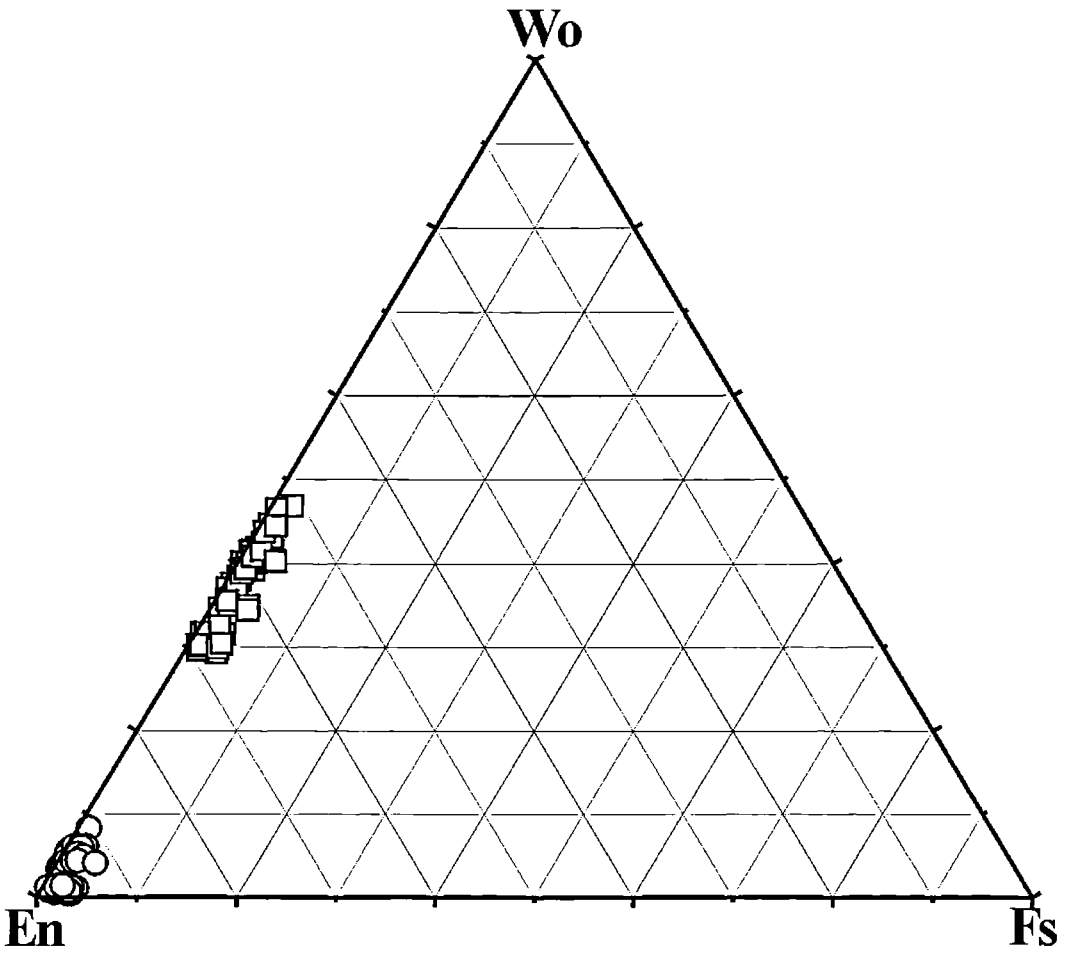

FIG. 6. Compositions of low-Ca (circles) and high-Ca (squares) pyroxenes in anorthite-rich chondrules in CR chondrites, in terms of mol% En (enstatite, $MgSiO_3$), Fs (ferrosilite, $FeSiO_3$) and Wo (wollastonite, $CaSiO_3$).

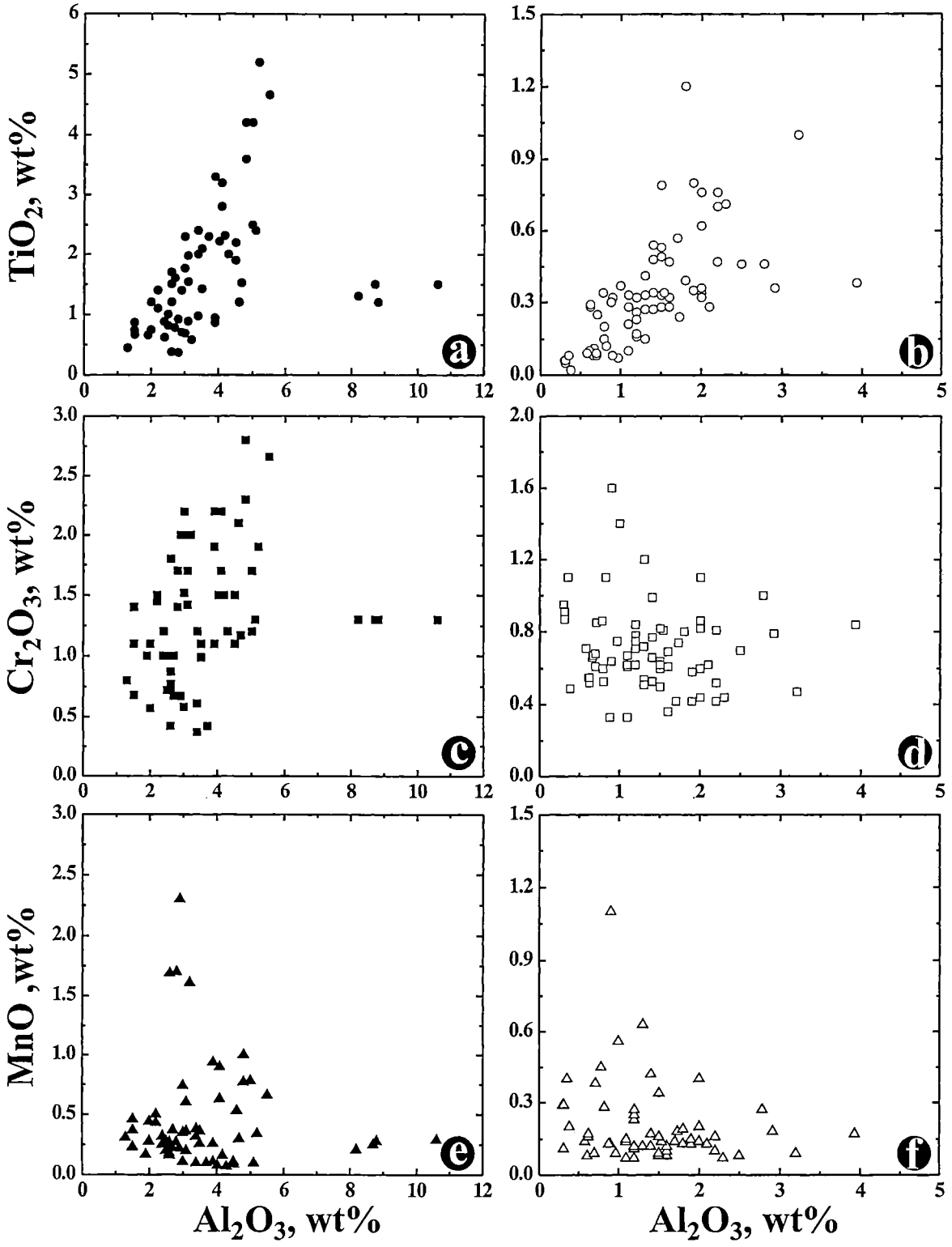

FIG. 7. Concentrations (in wt%) of TiO_2 (a, b), Cr_2O_3 (c, d) and MnO (e, f) *vs.* Al_2O_3 in high-Ca pyroxene (a, c, e) and low-Ca pyroxene (b, d, f) in anorthite-rich chondrules in CR chondrites.

TABLE 3. Average compositions of olivine in ARCs in CR chondrites.

Chondrite (pts)	chd	SiO_2	TiO_2	Al_2O_3	Cr_2O_3	FeO	MnO	MgO	CaO	Na_2O	K_2O	Total	Fa
PCA 91082,*16*	10	42.4	<0.04	0.04	0.60	1.0	0.21	56.2	0.23	<0.06	<0.04	100.7	1.0
	10	*0.10*	–	*0.02*	*0.10*	*0.1*	*0.10*	*0.17*	*0.02*	–	–	*0.1*	*0.1*
	17	41.9	<0.04	<0.03	0.60	1.5	0.16	55.6	0.18	<0.06	<0.04	100.0	1.5
MAC 87320, *9*	1	42.7	0.04	0.04	0.43	0.78	0.09	56.3	0.26	<0.06	<0.04	100.6	0.8
	1	*0.1*	*0.02*	*0.02*	*0.04*	*0.11*	*0.03*	*0.2*	*0.0*	–	–	*0.2*	*0.1*
El Djouf 001, *AB*	10	42.5	0.08	0.23	0.19	0.76	<0.07	56.2	0.57	<0.06	<0.04	100.6	0.8
	10	*0.1*	*0.05*	*0.12*	*0.17*	*0.45*	–	*0.4*	*0.18*	–	–	*0.2*	*0.4*
EET 92147, *7*	1	42.5	0.13	0.09	0.31	0.59	0.11	56.0	0.25	<0.06	<0.04	99.9	0.6
	1	*0.3*	*0.07*	*0.06*	*0.17*	*0.54*	*0.07*	*0.4*	*0.03*	–	–	*0.4*	*0.5*
GRA 92159, *18*	20	42.1	0.08	0.11	0.49	2.2	0.08	54.5	0.32	<0.06	<0.04	99.9	2.2
	20	*0.2*	*0.03*	*0.03*	*0.08*	*0.2*	*0.02*	*0.2*	*0.02*	–	–	*0.3*	*0.2*

Abbreviations: pts = thin section number; chd = chondrule.
Numbers in italics = 1σ.

phenocrysts in chondrule cores (Figs. 1d and 2d). Occasionally, olivine forms subrounded aggregates of grains associated with low-Ca pyroxene and abundant FeNi-metal nodules (Fig. 2a). Olivine in ARCs has forsteritic compositions ($Fa_{0.2–2.6}$) and is characterized by high concentrations of Cr_2O_3 (up to 0.9 wt% and a peak at about 0.4–0.6 wt%) and relatively low concentrations of other minor elements such as MnO, Al_2O_3 and CaO (Table 3; Fig. 8).

Plagioclase occurs as coarse (up to 50 μm in width) lath-shaped crystals in interstitial regions and as anhedral small grains closely intergrown with silica in chondrule mesostases (Figs. 1–4). It is also one of the major components of the CAI-like objects associated with ARCs (Figs. 3 and 5). Plagioclase is typically anorthitic in composition ($An_{85–100}$) with a peak at ~$An_{95–100}$; one of the ARCs in PCA 91082 contains relatively albitic plagioclase ($An_{70–80}$) (Table 4; Fig. 9a). Lath-shaped interstitial plagioclase tends to have more anorthitic compositions than plagioclase in the mesostasis; similar trends are observed for plagioclase in cores and peripheries of the chondrules. Plagioclase in the CR ARCs has rather high contents of MgO (up to 1.2 wt%) with a peak at about 0.8–0.9 wt% (Fig. 9b). Plagioclase in the CAI-like objects is nearly pure anorthite (Table 4).

Spinel is a minor mineral in ARCs and occurs as subhedral to euhedral grains enclosed in anorthite (Fig. 4a), and as anhedral grains in interstitial regions or as inclusions in forsterite phenocrysts (Fig. 2d). Spinel is one of the major minerals of the CAI-like objects associated with ARCs (Figs. 3 and 5). Spinel grains are FeO-poor (<1.7 wt%) and Cr-bearing (up to 8.7 wt% Cr_2O_3). Although spinel typically shows no within-grain compositional zoning, Cr concentrations can range broadly within a chondrule (Table 5; Fig. 3).

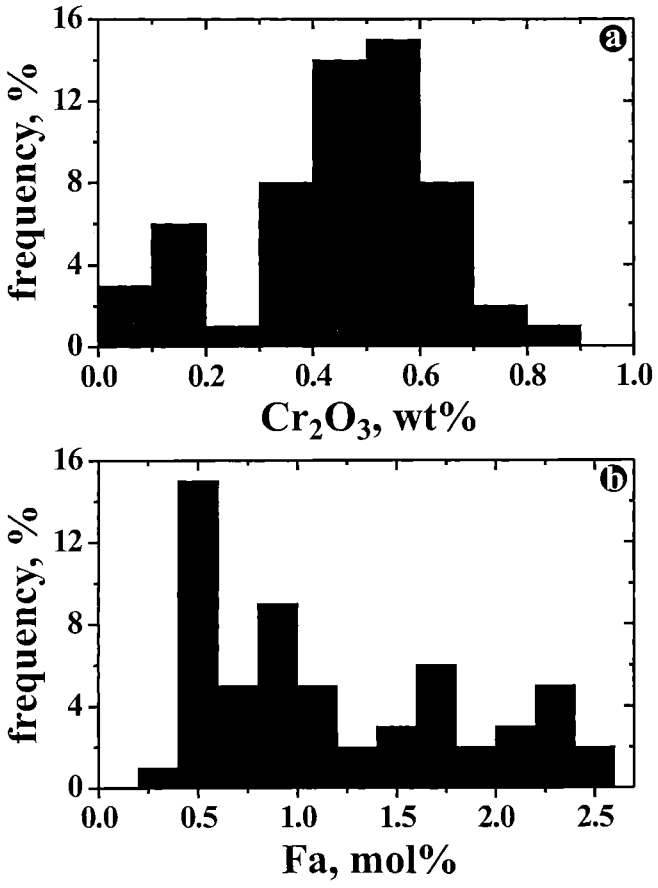

FIG. 8. Histograms of Cr_2O_3 (wt%) (a) and fayalite (Fa, Fe_2SiO_4, mol%) contents (b) in olivine in anorthite-rich chondrules in CR chondrites.

TABLE 4. Representative microprobe analyses of plagioclase in ARCs in CR and CH chondrites.

Chondrite (pts)	chd	pos	SiO_2	TiO_2	Al_2O_3	Cr_2O_3	FeO	MnO	MgO	CaO	Na_2O	K_2O	Total	An	Ab
EET 92042, 22	1	lath	44.9	0.04	34.8	<0.06	0.28	<0.07	0.62	19.5	0.40	<0.04	100.6	96.4	3.6
	1	*1.9*	*0.03*	*1.5*	–	*0.27*	–	*0.31*	*0.7*	*0.32*	–	*0.2*	*2.9*	*2.9*	
	1	mes	47.2	0.09	33.1	<0.06	0.33	<0.07	0.69	18.1	1.0	<0.04	100.6	90.9	9.0
	1	1.0	0.05	0.7	–	0.25	–	0.06	0.6	0.2	–	0.4	2.3	2.2	
PCA 91082, 20	9	lath	51.0	0.05	30.5	<0.06	0.95	0.10	0.59	14.7	2.9	0.06	100.9	73.4	26.2
	9	*0.8*	*0.02*	*0.4*	–	*1.3*	*0.02*	*0.03*	*0.5*	*0.3*	*0.01*	*0.3*	*2.6*	*2.6*	
PCA 91082, 16	10	lath	47.5	0.05	32.0	<0.06	0.25	<0.07	0.96	18.2	0.59	<0.04	99.7	94.4	5.5
	10	*0.5*	*0.02*	*0.6*	–	*0.26*	–	*0.11*	*0.4*	*0.15*	–	*0.3*	*1.5*	*1.5*	
MAC 87320, 9	1	core	47.5	0.04	32.6	<0.06	0.23	<0.07	0.99	18.7	0.31	<0.04	100.4	97.1	2.9
	1	*0.4*	*0.02*	*0.2*	–	*0.26*	–	*0.06*	*0.3*	*0.1*	–	*0.2*	*1.1*	*1.1*	
	1	rim	47.7	0.05	32.6	<0.06	0.23	<0.07	0.89	18.5	0.44	<0.04	100.4	95.8	4.1
	1	*0.4*	*0.02*	*0.4*	–	*0.08*	–	*0.06*	*0.3*	*0.1*	–	*0.3*	*1.2*	*1.2*	
El Djouf 001, AB	10	core	45.7	<0.04	33.7	<0.06	0.12	<0.07	1.0	19.5	0.20	<0.04	100.3	98.1	1.9
El Djouf 001, AB	10	*2.8*	–	*2.3*	–	*1.18*	–	*0.06*	*1.4*	*0.08*	–	*2.5*	*0.8*	*0.8*	
El Djouf 001, AB	10	rim	46.4	0.04	33.2	<0.06	0.26	<0.06	1.1	19.1	0.3	<0.04	100.4	97.1	2.9
Acfer 182, AB	1	CAI	42.6	0.15	36.4	0.10	0.29	<0.07	0.27	19.9	<0.06	<0.04	99.7	100.0	0.0
	1	chd	45.6	0.12	34.0	<0.06	0.33	<0.07	0.61	18.9	0.45	–	100.1	95.9	4.1
EET 92147, 7	1	CAI	43.8	0.05	35.7	<0.06	0.21	<0.07	0.52	19.9	0.09	<0.04	100.3	99.1	0.8
	1	*0.6*	*0.03*	*0.6*	–	*0.23*	–	*0.11*	*0.3*	*0.07*	–	*0.3*	*0.7*	*0.7*	
	1	chd	44.5	0.04	35.1	<0.06	0.66	<0.07	0.61	19.5	0.43	<0.04	100.8	96.1	3.8
	1	*0.6*	*0.02*	*0.4*	–	*0.66*	–	*0.04*	*0.4*	*0.19*	–	*0.4*	*1.7*	*1.7*	

Numbers in italics = 1σ.

Abbreviations: pts = thin section number; lath = coarse-grained plagioclase laths; mes = fine-grained plagioclase in mesoastsis; chd = chondrule; CAI = relic calcium-aluminum-rich inclusion; pos = position.

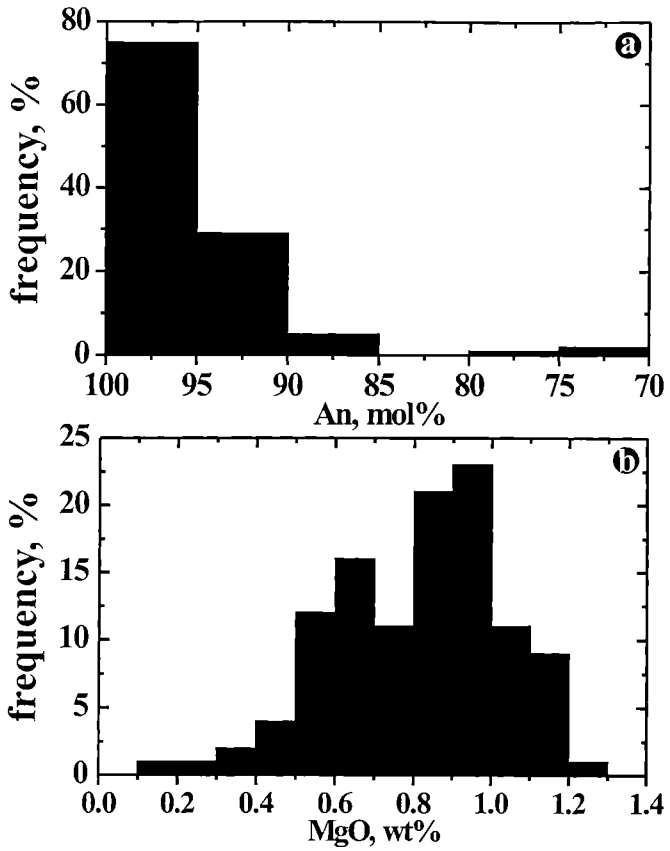

FIG. 9. Histograms of anorthite (An, $CaAl_2Si_2O_8$, mol%) (a) and MgO contents (wt%) in plagioclase in anorthite-rich chondrules in CR chondrites.

FeNi-metal nodules are rather common in ARCs (Figs. 1–3). They have kamacitic compositions and are compositionally uniform within a chondrule (Table 6). In contrast to typical ferromagnesian chondrules, the mesostasis in ARCs is crystalline and silica-rich; it consists of anorthitic plagioclase, silica, and high-Ca pyroxene (Figs. 1, 2, and 4).

The irregularly-shaped CAI-like objects associated with ARCs consist of anorthite, spinel, diopsidic pyroxene (only in the Acfer 087 chondrule) and minor forsterite (Figs. 3 and 5). In contrast to the host chondrules, these objects contain no low-Ca pyroxene, FeNi-metal nodules or mesostasis, and probably represent relic CAIs (see "Discussion").

Anorthite-Rich Chondrule with Relic Calcium-Aluminum-Rich Inclusion in Acfer 182

The only ARC found in the CH chondrite Acfer 182 is mineralogically similar to the pyroxene-rich ARCs in CR chondrites; it consists of Al-Ti-Cr-rich low-Ca and high-Ca pyroxenes, anorthite (An_{96}), FeNi-metal nodules, and crystalline silica-anorthite-high-Ca pyroxene mesostasis (Fig. 10). It contains a relic CAI composed of several spinel cores surrounded by anorthite ($An_{99.5}$); rare inclusions of perovskite occur in spinel. The relic origin of the CAI is supported by oxygen-isotopic studies (Krot *et al.*, 1999b). Spinel of the relic CAI is enriched in ^{16}O ($\delta^{18}O = -37‰$, $\delta^{17}O = -40‰$) relative to anorthite ($\delta^{18}O = -13‰$, $\delta^{17}O = -15‰$); chondrule pyroxenes have heavy O-compositions ($\delta^{18}O = +8‰$, $\delta^{17}O = +4‰$).

DISCUSSION

Crystallization History of Anorthite-Rich Chondrules

Our petrographic observations suggest that in olivine- and pyroxene-rich ARCs (Figs. 1 and 2), forsterite and low-Ca pyroxenes phenocrysts crystallized first, followed by interstitial pigeonite, augite and anorthite; silica-anorthite-augite mesostasis crystallized last. Rare spinel grains observed as inclusions in forsterite phenocrysts (Fig. 2d) and in coarse anorthite laths (Fig. 4) probably crystallized first; the relic origin of some spinel grains cannot excluded, however. In a few ARCs exceptionally rich in anorthite (Fig. 4), crystallization

TABLE 5. Microprobe analyses of spinel in ARCs in CR and CH chondrites.

an.	1	2	3	4	5	6	7
SiO_2	0.07	0.12	0.06	0.12	0.25	0.07	0.09
TiO_2	0.40	0.54	0.69	0.20	0.22	0.18	1.1
Al_2O_3	72.2	66.7	71.5	71.6	70.8	63.7	69.5
Cr_2O_3	0.15	5.1	0.72	0.44	1.1	8.7	0.61
FeO	0.71	0.69	0.28	0.48	0.51	1.7	1.6
MnO	0.07	<0.07	0.09	0.08	<0.07	<0.07	0.2
MgO	27.3	26.6	27.3	27.8	27.7	25.3	26.8
CaO	0.05	0.09	0.05	0.04	0.03	<0.03	0.09
Na_2O	<0.06	<0.06	<0.06	<0.06	<0.06	<0.06	<0.06
K_2O	<0.04	<0.04	<0.04	<0.04	<0.04	<0.04	<0.04
Total	100.9	99.9	100.7	100.8	100.6	99.6	100.0

an. = analysis number; an. 1, 2 = EET 92041, 2 (chd #1); an. 3 = EET 92147, 7 (chd #1); an. 4, 5 = El Djouf 001, AB (chd #10); an. 6 = GRA 92159, 18 (chd #13); an. 7 = Acfer 182, AB (chd #1).

TABLE 6. Average compositions of FeNi-metal grains in ARCs in CR chondrites.

Chondrite, *pts*	chd	Fe	Ni	Co	Cr	Si	S	P	Total
PCA 91082, *16*	10	92.9	5.4	0.36	0.52	0.09	<0.03	0.41	99.7
	10	*0.6*	*0.2*	*0.01*	*0.10*	*0.03*	–	*0.0*	*0.5*
	17	92.8	6.3	0.39	0.28	0.07	<0.03	0.30	100.2
	17	*0.6*	*0.4*	*0.02*	*0.07*	*0.02*	–	*0.07*	*0.5*

Numbers in italics = 1σ.
Abbreviations: pts = thin section number; chd = chondrule.

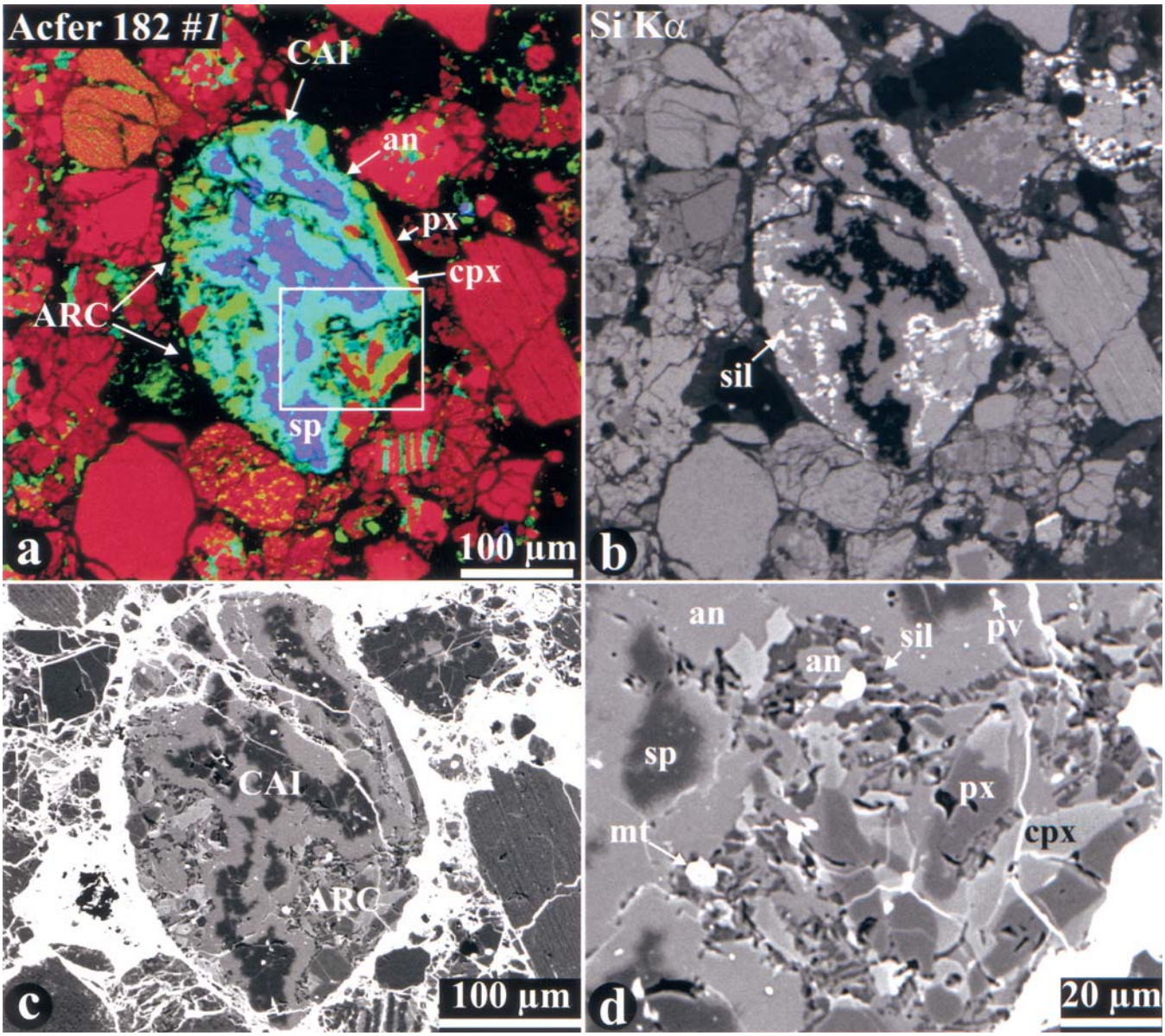

FIG. 10. Combined x-ray elemental map in Mg (red), Ca (green) and Al Kα (blue) (a), elemental map in Si Kα (b) and backscattered electron images (c, d) of the anorthite-rich chondrule #1 (ARC) containing relic refractory inclusion (CAI) in the CH chondrite Acfer 182. The CAI consists of irregularly-shaped spinel cores surrounded by anorthite; tiny perovskite (pv) inclusions occur in spinel. The chondrule portion consists of low-Ca pyroxene, high-Ca pyroxene, FeNi-metal nodules and silica-rich crystalline mesostasis composed of silica, anorthite and high-Ca pyroxene. Region outlined in (a) is shown in detail in (d). White veins in (c) and (d) are veins of terrestrial weathering products.

of anorthite may have predated crystallization of mafic silicates. The inferred crystallization sequence is consistent with the evolution of the chemical compositions of the chondrule pyroxenes: concentrations of Cr, Al, and Ti in pyroxenes increase from phenocrysts to interstitial to mesostasis. The observed enrichment in Cr, Al, and Ti and Na of pyroxenes and plagioclase in mesostasis relative to the interstitial pyroxenes and plagioclase suggests that fractional crystallization played an important role during crystallization of the ARC melts (Tables 2 and 4).

Two of the ARCs in CR chondrites contain inclusions of CAI-like objects which are mineralogically different from the host chondrules, suggesting their relic origin. Both CAIs contain forsterite closely intergrown with spinel grains (Figs. 3 and 5). Although forsterite associated with refractory inclusions is not uncommon in CR chondrites (*e.g.*, amoeboid olivine aggregates (AOAs) and forsterite rims around CAIs), the forsterite-bearing CAIs (in which forsterite would crystallize from the CAI melt) in CR chondrites have not been found yet (Weber and Bischoff, 1997; Weisberg, unpubl. data; Krot, unpubl. data). Moreover, rare forsterite-bearing CAIs previously described only in CV carbonaceous chondrites are mineralogically different from those inside CR ARCs (Blander and Fuchs, 1975; Dominik *et al.*, 1978; Clayton *et al.*, 1984; Wark *et al.*, 1987; Krot *et al.*, 2000a). Based on these observations, we infer that although the CAI-like objects in CR ARCs are relic, they probably experienced melting during the chondrule-forming episode, which resulted in crystallization of forsterite grains. A degree of mixing between the CAI and chondrule melts could be possibly inferred from future O-isotopic studies of these chondrules.

The CAI-like object in Acfer 182 is not only mineralogically, but also isotopically different from the host chondrule, strongly indicating its relic origin (Krot *et al.*, 1999b). At the same time, anorthite surrounding ^{16}O-rich spinel cores is closely intergrown with the chondrule silicates (Fig. 10); its O-isotopic compositions are intermediate between those of the host chondrule and CAI spinel (see "Anorthite-Rich Chondrule with Relic Calcium-Aluminum-Rich Inclusion in Acfer 182"). Based on these observations, we infer that the relic CAI in the Acfer 182 chondrule experienced some melting and isotopic equilibration with the chondrule melt. These data will be discussed in more detail in a later paper.

Some of the ARCs contain regions that are texturally and mineralogically similar to type I chondrules and could be relic in origin as well (Fig. 2a). Similar observations have previously been reported from ARCs in CO (Jones and Brearley, 1994; Hutcheon and Jones, 1995) and CV carbonaceous chondrites (Hutcheon *et al.*, 2000; Krot, 2000).

ARCs from CO and CV chondrites typically show evidence for post-crystallization alteration that resulted in replacement of anorthite and silica by nepheline and ferrosilite-rich pyroxenes (Krot, 2000). No alteration minerals were found in the CR and CH ARCs underlining their primitive nature.

Similarities and Differences Between Anorthite-Rich Chondrules in CR and Other Carbonaceous Chondrite Groups

Our mineralogical observations indicate that ARCs in CR and CH chondrites have similar primary mineralogies to those in CO (Jones and Brearley, 1994; Hutcheon and Jones, 1995), CV and unique carbonaceous chondrites Acfer 094 (Hutcheon *et al.*, 2000; Krot, 2000; Marhas *et al.*, 2000) and Adelaide (Krot, unpubl. data). The similar mineralogical features, probably indicating similar precursors and crystallization histories, include (1) dominant pyroxene-rich compositions; (2) high concentrations of Al, Ti and Cr in pyroxenes; (3) crystalline silica-anorthite-augite mesostasis; (4) presence of type I chondrule-like regions composed of forsterite, low-Ca pyroxene and abundant FeNi-metal nodules; and (5) common occurrences or relic refractory inclusions composed of spinel, anorthite, ±diopside and ±forsterite.

However, there are some differences in forsterite and plagioclase compositions in ARCs from the CR and CV chondrites (data for the CO ARCs are scarce). Forsterite grains in ARCs in CR chondrites have higher average concentrations of Cr_2O_3 (0.6 ± 0.1 wt%) than those in the CV ARCs (0.2 ± 0.1 wt%) (Krot, 2000). Most plagioclase grains in the CR ARCs are nearly pure anorthite ($An_{96\pm2}$), whereas those in the CV ARCs have more albitic compositions ($An_{83\pm5}$) (Krot, 2000). The differences in plagioclase compositions may have resulted from the secondary Fe-Na-metasomatic alteration experienced by all components of the CV chondrites (Krot *et al.*, 1998). Although the presence of nepheline and ferrosilite in most CV ARCs is consistent with this interpretation, no correlation between plagioclase composition and a degree of its replacement by secondary nepheline was found (Krot, 2000). The differences in forsterite compositions could be primary, since the enrichment of chondrule silicates in Cr is a characteristic feature of the CR clan of chondritic meteorites (Weisberg *et al.*, 1995; Krot *et al.*, 2001, unpubl. data). Alternatively, chromium could have diffused out during mild thermal metamorphism in CV chondrites. We infer that the CV and CR ARCs formed from precursor materials that originated in the CV and CR ARC-forming regions, respectively.

Anorthite-Rich and Type I Chondrules in CR Chondrites: Formation at Different Ambient Nebular Temperatures?

Krot *et al.* (2000b) discovered that many type I chondrules in CR chondrites are surrounded by silica-rich igneous rims; these rims are enriched in moderately volatile elements such as Si, Mn, Cr, Na, and K relative to the host chondrules; both the layered chondrules and their igneous rims are highly depleted in S. Krot *et al.* (2000b; 2001, unpubl. data) inferred that the layered type I chondrules in CR chondrites formed at high ambient nebular temperatures (about 1100–1000 K), while condensation of the major chondrule-forming elements was

still incomplete. These chondrules were isolated from the hot nebular gas before condensation of S, possibly by removal into a cold nebular region.

The anorthite-rich chondrules in CR chondrites lack silica-rich igneous rims (Figs. 1–6) and their plagioclases are highly depleted in Na and K relative to the mesostases of the layered type I chondrules (Fig. 11). These observations might indicate that ARCs in CR chondrites formed at higher ambient nebular temperatures than the layered type I chondrules and were largely absent from the region where typical type I chondrules formed. The presence of the crystalline mesostases in ARCs, contrary to the glassy mesostases in type I chondrules (Jones and Scott, 1989; Krot *et al.*, 2000b), is also consistent with the different thermal histories of these chondrule types.

Genetic Relationships between Anorthite-Rich Chondrules, Type I Chondrules, Amoeboid Olivine Aggregates and Calcium-Aluminum-Rich Inclusions

MacPherson and Russell (1997) concluded that Al-rich chondrules are "not intermediate in an evolutionary sense, between known CAIs and chondrules, but closely related to normal ferromagnesian chondrules, either by addition of anorthite-like component to chondrule precursors, or, possibly, in some cases, by volatilization of chondrule or chondritic material of unusual oxygen-isotopic composition". These authors noted that if Al-rich compositions resulted from mixing of refractory material into chondrule precursor aggregates (*e.g.*, type IA), then the refractory component did not have the bulk-major-element composition of known CV, CO, or CM CAIs. Rather, the component largely had the composition of anorthite with minor amounts of spinel and Ti-bearing clinopyroxene. Although our observations are generally consistent with this conclusion, the relatively high abundances of moderately-volatile elements such as Si, Cr, and Mn in ARCs argues against volatilization during their formation. The presence of relic CAIs in ARCs suggests a genetic relationship between these classes of objects (Krot, 2000; this study). The latter conclusion is also supported by the discovery of the ^{16}O-rich ($\delta^{17}O = -34‰$, $\delta^{18}O = -30‰$) spinel grains in the Allende ARCs (Maruyama *et al.*, 1998a,b) and by volatility-controlled group II REE patterns of some of the ARCs (Misawa and Nakamura, 1988, 1996; Kring and Boynton, 1990).

Bulk chemical compositions of ARCs are rather similar to those of AOAs in carbonaceous chondrites and can be produced by addition of anorthite-rich material to AOAs (Fig. 12). The

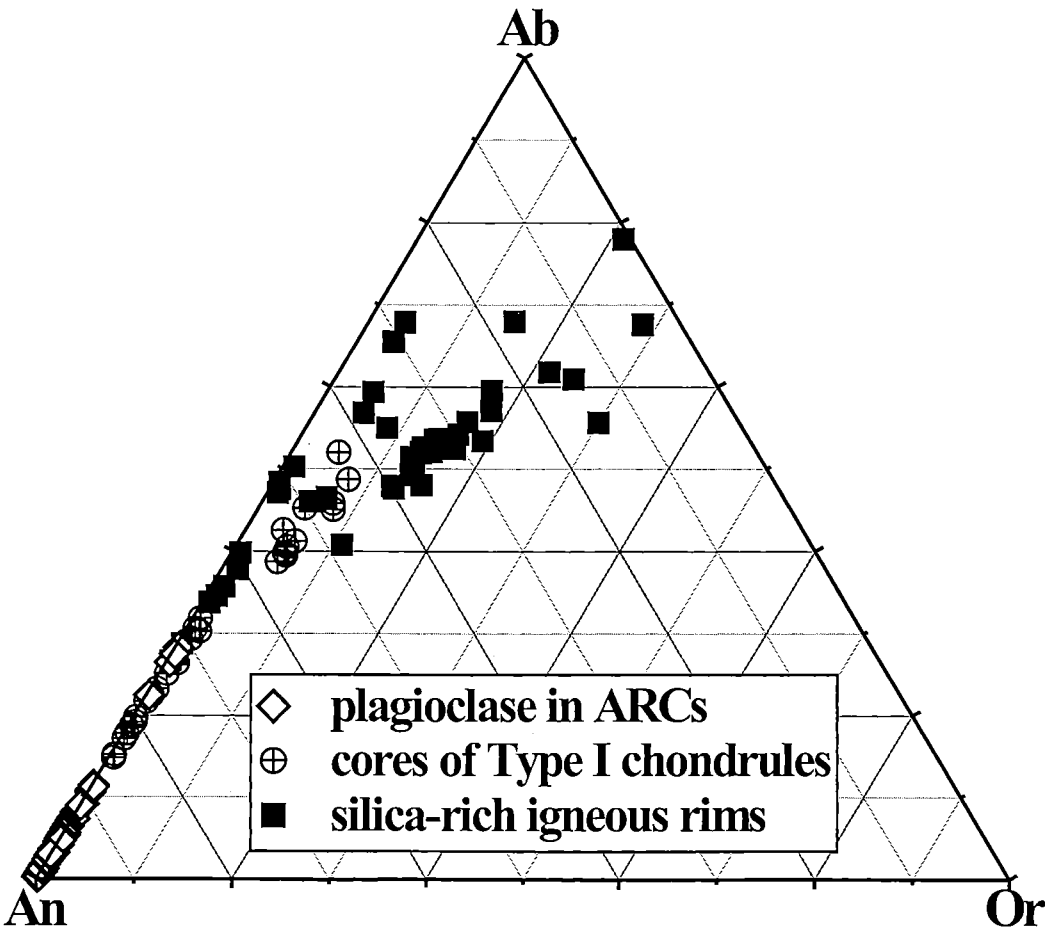

FIG. 11. Compositions of plagioclase in anorthite-rich chondrules and glassy mesostases in type I chondrules and silica-rich igneous rims around them in CR chondrites, in terms of mol% An (anorthite, $CaAl_2Si_2O_8$), Or (orthoclase, $KAlSi_3O_8$) and Ab (albite, $NaAlSi_3O_8$).

AOAs typically contain a refractory component mineralogically similar to the relic CAIs in ARCs and composed of anorthite, Al-Ti-diopside and spinel (Bar-Matthews *et al.*, 1979; Kornacki and Wood, 1984; Chizmadia and Rubin, 2000; Komatsu *et al.*, 2001). Although these observations indicate that some of the ARCs could have formed by remelting of AOAs or of associated refractory components, there are several arguments against this simple scenario. (1) AOAs are generally depleted in FeNi-metal, Mn, Cr, Na, and Si relative to ARCs; most of the ARCs are pyroxene-rich (Komatsu *et al.*, 2001). We note, however, that Cr- and Mn-rich forsterites were described in AOAs in CR chondrites (Weisberg *et al.*, 2001); metal-rich AOAs were found in Adelaide (Krot, unpubl. data). (2) The AOAs have more ^{16}O-rich isotopic compositions than the ARCs (Hiyagon and Hashimoto, 1998, 1999; Russell *et al.*, 2000; Krot and McKeegan, 2001). We note, however, that O-isotopes of the CR AOAs and ARCs have not been studied yet. (3) AOAs do not show evidence for being extensively melted; rather they are aggregates of solar nebula condensates that experienced high-temperature annealing (Komatsu *et al.*, 2001). We conclude that it is very unlikely that ARCs formed by melting of AOAs; more volatile and less ^{16}O-rich precursor material is required. The observed type I chondrule-like regions in some ARCs may support this conclusion (Fig. 2a).

Calcium-Aluminum-Rich Inclusions and Chondrule-Forming Regions: Placing the Formation Region of Anorthite-Rich Chondrules

It was recently suggested that refractory inclusions (CAIs and AOAs) and ferromagnesian chondrules formed in isotopically different regions separated in time or in space (*e.g.*, Shu *et al.*, 1996; McKeegan *et al.*, 1998; Krot *et al.*, 1999a,b, 2001; Fagan *et al.*, 2000a,b; Komatsu *et al.*, 2001). The CAI-forming regions were typically characterized by a "canonical" $^{26}Al/^{27}Al$ ratio of $\sim 5 \times 10^{-5}$ (*e.g.*, MacPherson *et al.*, 1995) and ^{16}O-rich isotope compositions ($\delta^{17}O$, $\delta^{18}O \approx -40‰$), whereas the chondrule-forming regions had $^{26}Al/^{27}Al$ ratios of $< 1.5 \times 10^{-5}$ (MacPherson *et al.*, 1995; Russell *et al.*, 1996, 1997a; Hutcheon *et al.*, 2000; Marhas *et al.*, 2000; Srinivasan *et al.*, 2000) and ^{16}O-poor isotope compositions ($\delta^{17}O$, $\delta^{18}O > -10‰$) (Russell *et al.*, 1997b, 2000; McKeegan *et al.*, 1998).

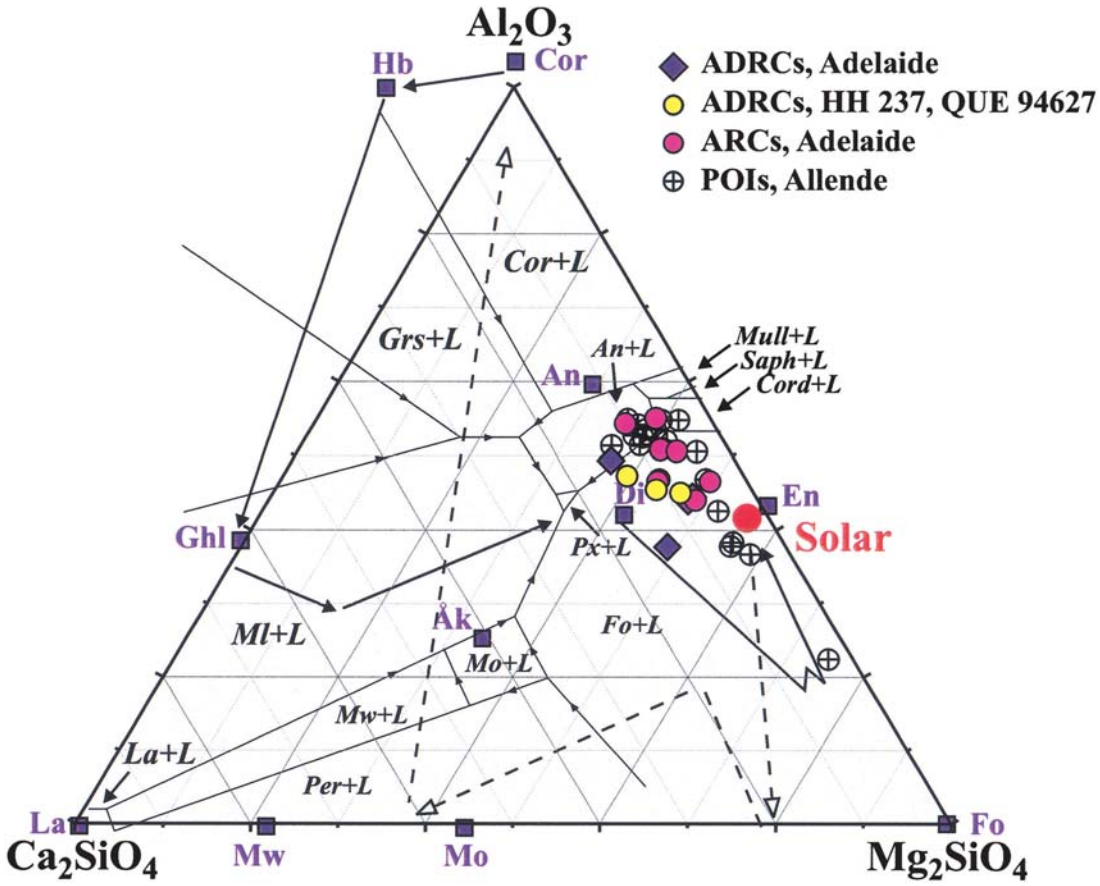

FIG. 12. Bulk compositions of CAIs, AOAs and ARCs in CR chondrites (data from Weber and Bischoff, 1997) and AOAs and POIs in CV chondrites (data from Sheng *et al.*, 1991 and McSween, unpubl. data) projected from spinel onto the plane larnite (La)–forsterite (Fo)–corundum (Cor), together with the spinel-saturated liquidus relationships in this system; solid vectors show calculated trajectory for bulk condensed solids during equilibrium condensation; dashed vectors show experimentally determined compositions of liquids during melt evaporation (after MacPherson and Huss, 2000).

The majority of CAIs show no evidence for being present in the regions where typical ferromagnesian (type I and type II) chondrules formed at the time of chondrule formation (Krot *et al.*, 1999a,b). The following observations support this conclusion: (1) In contrast to ferromagnesian chondrules, the CAIs generally show evidence for gas–solid and/or gas–liquid reactions which resulted in replacement of melilite and spinel by anorthite and Al-diopside, formation of Wark–Lovering rims, and mass-dependent isotope fractionation. These observations suggest that CAIs stayed at high temperatures for a longer period of time than typical chondrules. The estimated cooling rates of igneous (type B) CAIs (1–10 K h^{-1}) are much slower than those inferred for typical ferromagnesian chondrules (100–1000 K h^{-1}) (*e.g.*, Davis and MacPherson, 1996; Connolly and Love, 1998; Jones *et al.*, 2000; Rubin, 2000). (2) Most CAIs are surrounded by Wark–Lovering rims, which are absent around chondrules. Since the liquidus temperatures of most CAIs are generally lower or comparable to those of type I chondrules (Stolper, 1982; Jones *et al.*, 2000), and if the CAIs were present in the chondrule-forming regions, they would have melted and their Wark–Lovering rims would have been destroyed; this is generally not the case. (3) Compound CAI-chondrule objects and coarse-grained igneous rims around CAIs are absent; relic CAIs in ferromagnesian chondrules are extremely rare (Srinivasan and Bischoff, 1998; Krot *et al.*, 1999b). (4) The large depletions of the refractory inclusions in moderately volatile elements such as Mn, Cr, Na, and K suggest that the CAIs were isolated from the nebular gas at higher ambient temperatures than the ferromagnesian chondrules.

The mineralogy, bulk chemistry and O-isotopic compositions of the ARCs in carbonaceous chondrites may indicate that their formation region(s) was closer to that of the refractory inclusions than to that of ferromagnesian chondrules. (1) The presence of crystalline silica-anorthite-augite mesostases in the ARCs may suggest that they cooled slower than typical type I chondrules. (2) The depletion of ARCs in Na and K compared to type I chondrules may suggest that the ARCs formed at higher ambient temperatures than the type I chondrules. (3) Oxygen-isotopic compositions of ARCs are intermediate of those of CAIs and type I chondrules. (4) In contrast to ferromagnesian chondrules, the relic CAIs are commonly found in the ARCs.

We conclude that ARCs in CR and CH carbonaceous chondrites may have formed at high ambient nebular temperatures by melting of reduced chondrule precursors (olivine, pyroxenes, FeNi-metal) mixed with the refractory materials, including relic anorthite-rich CAIs. The ARCs may have formed in the region intermediate between the regions where CAIs and ferromagnesian chondrules originated.

Acknowledgements–This work was supported by NASA grants NAG 5-10610 (A. N. Krot, P. I.) and NAG 5-4212 (K. Keil, P. I.). We thank the Antarctic Meteorite Working Group (NASA, Johnson Space Center), American Museum of Natural History (New York), Addi Bischoff (Institut für Planetologie, Münster) and Ansgar Greshake (Institut für Mineralogie, Humboldt Universität, Berlin) for providing polished thin sections of the meteorites studied. We thank Sara S. Russell, Harold C. Connolly, Jr. and Paul H. Warren for thoughtful reviews. This is Hawaii Institute of Geophysics and Planetology publication No. 1188 and School of Ocean and Earth Science and Technology publication No. 5889.

Editorial handling: P. H. Warren

REFERENCES

BAR-MATTHEWS M., MACPHERSON G. J. AND GROSSMAN L. (1979) An SEM-petrographic study of amoeboid olivine aggregates in Allende (abstract). *Meteoritics* **14**, 342.

BISCHOFF A. AND KEIL K. (1984) Al-rich objects in ordinary chondrites: Related origin of carbonaceous and ordinary chondrites and their constituents. *Geochim. Cosmochim. Acta* **48**, 693–709.

BISCHOFF. A., SPETTEL B. AND PALME H. (1985) Trace elements in Al-rich chondrules from Ybbsitz (H4) (abstract). *Meteoritics* **20**, 609–610.

BISCHOFF A. *ET AL.* (1993) Paired Renazzo-type (CR) carbonaceous chondrites from the Sahara. *Geochim. Cosmochim. Acta* **57**, 1587–1603.

BLANDER M. AND FUCHS L. H. (1975) Calcium-aluminum-rich inclusions in the Allende meteorite: Evidence for a liquid origin. *Geochim. Cosmochim. Acta* **39**, 1605–1619.

CHIZMADIA L. J. AND RUBIN A. E. (2000) Petrology and origin of amoeboid olivine inclusions in CO3 chondrites (abstract). *Lunar Planet. Sci.* **31**, #1494, Lunar and Planetary Institute, Houston, Texas, USA (CD-ROM).

CLAYTON R. N., MACPHERSON G. J., HUTCHEON I. D., DAVIS A. M., GROSSMAN L., MAYEDA T. K., MOLINI-VELSKO C. A., ALLEN J. M. AND EL GORESY A. (1984) Two forsterite-bearing FUN inclusions in the Allende meteorite. *Geochim. Cosmochim. Acta* **48**, 535–548.

CONNOLLY H. C., JR. AND LOVE S. G. (1998) The formation of chondrules; petrologic tests of the shock wave model. *Science* **280**, 62–67.

DAVIS A. M. AND MACPHERSON G. J. (1996) Thermal processing in the solar nebular: Constraints from refractory inclusions. In *Chondrules and the Protoplanetary Disk* (eds. R. H. Hewins, R. H. Jones and E. R. D. Scott), pp. 71–76. Cambridge Univ. Press, Cambridge, U.K.

DOMINIK B., JESSBERGER E. K., STAUDACHER T., NAGEL K. AND EL GORESY A. (1978) A new type of white inclusion in Allende; petrography, mineral chemistry, ^{40}Ar-^{39}Ar ages, and genetic implications. *Proc. Lunar Planet. Sci. Conf.* **9th**, 1249–1266.

FAGAN T. J., KROT A. N. AND KEIL K. (2000a) Calcium, aluminum-rich inclusions in enstatite chondrites (I): Mineralogy and textures. *Meteorit. Planet. Sci.* **35**, 771–783.

FAGAN T. J., MCKEEGAN K. D., KROT A. N. AND KEIL K. (2000b) Calcium-aluminum-rich inclusions in enstatite chondrites (2): Oxygen isotopes. *Meteorit. Planet. Sci.* **36**, 223–230.

GOSWAMI J. N. AND VANHALA H. A. T. (2000) Extinct radionuclides and the origin of the solar system. In *Protostars and Planets IV* (eds. M. Mannings, A. P. Boss and S. S. Russell), pp. 963–994. Univ. Arizona Press, Tucson, Arizona, USA.

GOSWAMI J. N., SRINIVASAN G. AND ULYANOV A. A. (1994) Ion microprobe studies of Efremovka CAIs: I. Magnesium isotope composition. *Geochim. Cosmochim. Acta* **58**, 431–447.

GUAN Y., MCKEEGAN K. D. AND MACPHERSON G. J. (2000a) Oxygen isotopes of CAIs from unequilibrated enstatite chondrites: Characteristics and implications (abstract). *Lunar Planet. Sci.* **31**, #1744, Lunar and Planetary Institute, Houston, Texas, USA (CD-ROM).

GUAN Y., HUSS G. R., MACPHERSON G. J. AND WASSERBURG G. J. (2000b) Calcium-aluminum-rich inclusions from enstatite chondrites; indigenous or foreign? *Science* **289**, 1330–1333.

HIYAGON H. AND HASHIMOTO A. (1998) An ion microprobe study of oxygen isotopes in Murchison (CM2) and Yamato 86009 (CV3) chondrites: Discovery of olivine inclusions with large ^{16}O-excess (abstract). *Meteorit. Planet. Sci.* **33 (Suppl.)**, A68–A69.

HIYAGON H. AND HASHIMOTO A. (1999) An ion microprobe study of oxygen isotopes in various types of inclusions in Y-82050 (CO3), ALHA77307 (CO3) and Y-86009 (CV3) chondrites (abstract). *Lunar Planet. Sci.* **30**, #1319, Lunar and Planetary Institute, Houston, Texas, USA (CD-ROM).

HSU W., HUSS G. R. AND WASSERBURG G. J. (2000) Compound CAI and multi-stage formation: Evidence of ^{26}Al abundances from the Allende 5241 CAI (abstract). *Lunar Planet. Sci.* **31**, #1734, Lunar and Planetary Institute, Houston, Texas, USA (CD-ROM).

HUSS G. R., MACPHERSON G. J., WASSERBURG G. J., RUSSELL S. S. AND SRINIVASAN G. (2001) Aluminium-26 in calcium-aluminium-rich inclusions and chondrules from unequilibrated ordinary chondrites. *Meteorit. Planet. Sci.* **36**, 975–999.

HUTCHEON I. D. AND HUTCHISON R. (1989) Evidence from the Semarkona ordinary chondrite for ^{26}Al heating of small planets. *Nature* **337**, 238–241.

HUTCHEON I. D. AND JONES R. H. (1995) The ^{26}Al-^{26}Mg record of chondrules: Clues to nebular chronology (abstract). *Lunar Planet. Sci.* **26**, 647–648.

HUTCHEON I. D., KROT A. N. AND ULYANOV A. A. (2000) ^{26}Al in anorthite-rich chondrules in primitive carbonaceous chondrites: Evidence chondrules post-date CAI (abstract). *Lunar Planet. Sci.* **31**, #1869, Lunar and Planetary Institute, Houston, Texas, USA (CD-ROM).

ITO M., YURIMOTO H. AND NAGASAWA H. (2000) A study of Mg and K isotopes in Allende CAIs: Implication to the time scale for the multiple heating processes (abstract). *Lunar Planet. Sci.* **31**, #1600, Lunar and Planetary Institute, Houston, Texas, USA (CD-ROM).

JONES R. H. AND BREARLEY A. (1994) Reduced, plagioclase-rich chondrules in the Lance and Kainsaz CO3 chondrites (abstract). *Lunar Planet. Sci.* **25**, 641–642.

JONES R. H. AND SCOTT E. R. D. (1989) Petrology and thermal history of type IA chondrules in the Semarkona (LL3.0) chondrite. *Proc. Lunar Planet. Sci. Conf.* **19th**, 523–536.

JONES R. H., LEE T., CONNOLLY H. C., JR., LOVE S. G. AND SHANG H. (2000) Formation of chondrules and CAIs: Theory *vs.* Observation. In *Protostars and Planets IV* (eds. M. Mannings, A. P. Boss and S. S. Russell), pp. 927–962. Univ. Arizona Press, Tucson, Arizona, USA.

KITA N., NAGAHARA H., TOGASHI S. AND MORISHITA Y. (2000) A short duration of chondrule formation in the solar nebula; evidence from ^{26}Al in Semarkona ferromagnesian chondrules. *Geochim. Cosmochim. Acta* **64**, 3913–3922.

KOMATSU M., KROT A. N., PETAEV M. I., ULYANOV A. A., KEIL K. AND MIYAMOTO M. (2001) Mineralogy and petrography of amoeboid olivine agggregates from the reduced CV3 chondrites Efremovka, Leoville and Vigarano: Products of nebular condensation, accretion and annealing. *Meteorit. Planet. Sci.* **36**, 629–642.

KORNACKI A. S. AND WOOD J. A. (1984) Petrography and classification of Ca, Al-rich and olivine-rich inclusions in the Allende CV3 chondrite. *J. Geophys. Res.* **89**, B573–B587.

KRING D. A. AND BOYNTON W. V. (1990) Trace-element compositions of Ca-rich chondrules from Allende: Relationships between refractory inclusions and ferromagnesian chondrules (abstract). *Meteoritics* **25**, 377.

KRING D. A. AND HOLMEN B. A. (1988) Petrology of anorthite-rich chondrules in CV3 and CO3 chondrites (abstract). *Meteoritics* **23**, 282.

KROT A. N. (2000) Anorthite-rich chondrules from primitive carbonaceous chondrites: Genetic links between CAI and chondrules (abstract). *Meteorit. Planet. Sci.* **35 (Suppl.)**, A93.

KROT A. N. AND MCKEEGAN K. D. (2001) Oxygen-isotopic compositions of forsterite in an accretionary rim around Ca, Al-rich inclusion and in an amoeboid olivine aggregate from the reduced CV chondrite Efremovka and their significance (abstract). *Lunar Planet. Sci.* **32**, #2016, Lunar and Planetary Institute, Houston, Texas, USA (CD-ROM).

KROT A. N., PETAEV M. I., SCOTT E. R. D., CHOI B-G., ZOLENSKY M. E. AND KEIL K. (1998) Progressive alteration in CV3 chondrites: More evidence for asteroidal alteration. *Meteorit. Planet. Sci.* **33**, 1065–1085.

KROT A. N., SAHIJPAL S., MCKEEGAN K. D., WEBER D., ULYANOV A. A., PETAEV M. I., MEIBOM A. AND KEIL K. (1999a) Unique mineralogy and isotopic signatures of Ca-Al-rich inclusions from the CH chondrite Acfer 182 (abstract). *Meteorit. Planet. Sci.* **34 (Suppl.)**, A69.

KROT A. N., SAHIJPAL S., MCKEEGAN K. D., WEBER D., GRESHAKE A, ULYANOV A. A., HUTCHEON I. D. AND KEIL K. (1999b) Mineralogy, Al-Mg and oxygen isotope studies of the relic CAIs in chondrules (abstract). *Meteorit. Planet. Sci.* **34 (Suppl.)**, A68–A69.

KROT A. N., ULYANOV A. A. AND KEIL K. (2000a) Forsterite-bearing Ca,Al-rich inclusion from the reduced CV chondrite Efremovka (abstract). *Meteorit. Planet. Sci.* **35 (Suppl.)**, A93–A94.

KROT A. N., WEISBERG M. K., PETAEV M. I., KEIL K. AND SCOTT E. R. D. (2000b) High-temperature condensation signatures in type I chondrules from CR carbonaceous chondrites (abstract). *Lunar Planet. Sci.* **31**, #1470, Lunar and Planetary Institute, Houston, Texas, USA (CD-ROM).

KROT A. N., ULYANOV A. A., MEIBOM A. AND KEIL K. (2001) Forsterite-rich accretionary rims around calcium-aluminum-rich inclusions from the reduced CV3 chondrite Efremovka. *Meteorit. Planet. Sci.* **36**, 611–628.

LATOURRETTE T. AND HUTCHEON I. D. (1999) Mg diffusion in melilite: Thermal histories for CAIs and their parent bodies (abstract). *Lunar Planet. Sci.* **30**, #2003, Lunar and Planetary Institute, Houston, Texas, USA (CD-ROM).

LATOURRETTE T. AND WASSERBURG G. J. (1998) Mg diffusion in anorthite; implications for the formation of early solar system planetesimals. *Earth Planet. Sci. Lett.* **158**, 91–108.

LEE T., PAPANASTASSIOU D. A. AND WASSERBURG G. J. (1976) Demonstration of ^{26}Mg excess in Allende and evidence for ^{26}Al. *Geophys. Res. Lett.* **3**, 41–44.

MACPHERSON G. J. AND DAVIS A. M. (1993) A petrologic and ion microprobe study of a Vigarano Type B refractory inclusion: Evolution by multiple stages of alteration and melting. *Geochim. Cosmochim. Acta* **57**, 231–243.

MACPHERSON G. J. AND HUSS G. R. (2000) Convergent evolution of CAIs and chondrules: Evidence from bulk compositions and a cosmochemical phase diagram (abstract). *Lunar Planet. Sci.* **31**, #1796, Lunar and Planetary Institute, Houston, Texas, USA (CD-ROM).

MACPHERSON G. J. AND RUSSELL S. S. (1997) Origin of aluminum-rich chondrules: Constraints from major-element chemistry (abstract). *Meteorit. Planet. Sci.* **32 (Suppl.)**, A83.

MACPHERSON G. J., DAVIS A. M. AND ZINNER E. K. (1995) The distribution of aluminum-26 in the early solar system: A reappraisal. *Meteoritics* **30**, 365–386.

MARHAS K. K., HUTCHEON I. D., KROT A. N. AND GOSWAMI J. N. (2000) ^{26}Al in carbonaceous chondrite chondrules (abstract). *Meteorit. Planet. Sci.* **35 (Suppl.)**, A102.

MARUYAMA S., YURIMOTO H. AND SUENO S. (1998a) CAI related spinel in a compound chondrule: Evidence of O isotope (abstract).

Lunar Planet. Sci. **29**, #1342, Lunar and Planetary Institute, Houston, Texas, USA (CD-ROM).

MARUYAMA S., YURIMOTO H. AND SUENO S. (1998b) Spinel-bearing chondrules in the Allende meteorite (abstract). *Meteorit. Planet. Sci.* **33 (Suppl.)**, A98.

MCKEEGAN K. D., LESHIN L. A., RUSSELL S. S. AND MACPHERSON G. J. (1998) Oxygen isotope abundances in calcium-aluminum-rich inclusions from ordinary chondrites: Implications for nebular heterogeneity. *Science* **280**, 414–418.

MCKEEGAN K. D., GREENWOOD J. P., LESHIN L. A. AND COZARINSKY M. (2000a) Abundance of ^{26}Al in ferromagnesian chondrules of unequilibrated ordinary chondrites (abstract). *Lunar Planet. Sci.* **31**, #2009, Lunar and Planetary Institute, Houston, Texas, USA (CD-ROM).

MCKEEGAN K. D., CHAUSSIDON M. AND ROBERT F. (2000b) Incorporation of short-lived ^{10}Be in a calcium-aluminum-rich inclusion from the Allende meteorite. *Science* **289**, 1334–1337.

MISAWA K. AND NAKAMURA N. (1988) Highly fractionated rare-earth elements in ferromagnesian chondrules from the Felix (CO3) meteorite. *Nature* **334**, 47–49.

MISAWA K. AND NAKAMURA N. (1996) Origin of refractory precursor components of chondrules from carbonaceous chondrites. In *Chondrules and the Protoplanetary Disk* (eds. R. H. Hewins, R. H. Jones and E. R. D. Scott), pp. 99–105. Cambridge Univ. Press, Cambridge, U.K.

MOSTEFAOUI S., KITA N. T., NAGAHARA H., TOGASHI S. AND MORISHITA Y. (1999) Aluminum-26 in two ferromagnesian chondrules from a highly unequilibrated ordinary chondrite: Evidence of a short period of chondrule formation (abstract). *Meteorit. Planet. Sci.* **34 (Suppl.)**, A84.

PODOSEK F. A. AND CASSEN P. (1994) Theoretical, observational, and isotopic estimates of the lifetime of the solar nebula. *Meteoritics* **29**, 6–25.

RUBIN A. E. (2000) Petrologic, geochemical and experimental constraints on models of chondrule formation. *Earth Sci. Reviews* **50**, 3–27.

RUSSELL S. S., SRINIVASAN G., HUSS G. R., WASSERBURG G. J. AND MACPHERSON G. J. (1996) Evidence for wide spread ^{26}Al in the solar nebula and constraints for nebula time scales. *Science* **273**, 757–762.

RUSSELL S. S., HUSS G. R., MACPHERSON G. J. AND WASSERBURG G. J. (1997a) Early and late chondrule formation: New constraints for solar nebula chronology from ^{26}Al/^{27}Al in unequilibrated ordinary chondrites (abstract). *Lunar Planet. Sci.* **28**, 1209–1210.

RUSSELL S. S., LESHIN L. A., MCKEEGAN K. D. AND MACPHERSON G. J. (1997b) Oxygen isotope composition of aluminum-rich chondrules: Clues to their origin (abstract). *Meteorit. Planet. Sci.* **32 (Suppl.)**, A111–A112.

RUSSELL S. S., MACPHERSON G. J., LESHIN L. A. AND MCKEEGAN K. D. (2000) ^{16}O enrichments in aluminum-rich chondrules from ordinary chondrites. *Earth Planet. Sci. Lett.* **184**, 57–74.

SAHIJPAL S., GOSWAMI J. N., DAVIS A. M., GROSSMAN L. AND LEWIS R. S. (1998) A stellar origin for the short-lived nuclides in the early solar system. *Nature* **391**, 559–561.

SHENG Y. J., HUTCHEON I. D. AND WASSERBURG G. J. (1991) Origin of plagioclase-olivine inclusions in carbonaceous chondrites. *Geochim. Cosmochim. Acta* **55**, 581–599.

SHU F. H., SHANG H. AND LEE T. (1996) Toward an astrophysical theory of chondrites. *Science* **271**, 1545–1552.

SRINIVASAN G. AND BISCHOFF A. (1998) Magnesium-aluminum study of hibonites within a chondrule-like object from Sharps (H3) (abstract). *Meteorit. Planet. Sci.* **33 (Suppl.)**, A148.

SRINIVASAN G., RUSSELL S. S., MACPHERSON G. J., HUSS G. R. AND WASSERBURG G. J. (1996a) New evidence for ^{26}Al in CAI and chondrules from type 3 ordinary chondrites (abstract). *Lunar Planet. Sci.* **27**, 1257–1258.

SRINIVASAN G., SAHIJAPAL S., ULYANOV A. A. AND GOSWAMI J. N. (1996b) Ion microprobe studies of Efremovka CAIs: II. Potassium isotope composition and ^{41}Ca in the early solar system. *Geochim. Cosmochim. Acta* **60**, 1823–1835.

SRINIVASAN G., KROT A. N. AND ULYANOV A. A. (2000) Al-Mg systematics in anorthite-rich chondrules and calcium-aluminum inclusions from the reduced CV chondrite Efremovka (abstract). *Meteorit. Planet. Sci.* **35 (Suppl.)**, A151–A152.

STOLPER E. (1982) Crystallization sequences of Ca-Al-rich inclusions from Allende: An experimental study. *Geochim. Cosmochim. Acta* **46**, 2159–2180.

VANHALA H. A. T. AND BOSS A. P. (2000) Injection of radioactivities into the forming solar system (abstract). *Lunar Planet. Sci.* **31**, #1061, Lunar and Planetary Institute, Houston, Texas, USA (CD-ROM).

WADHWA M. AND RUSSELL S. S. (2000) Timescales of accretion and differentiation in the early solar system: The meteoritic evidence. In *Protostars and Planets IV* (eds. V. M. Mannings, A. P. Boss and S. S. Russell), pp. 995–1018. Univ. Arizona Press, Tucson, Arizona, USA.

WARK D. A., BOYNTON W. V., KEAYS R. R. AND PALME H. (1987) Trace element and petrologic clues to the formation of forsterite-bearing Ca-Al-rich inclusions in the Allende meteorite. *Geochim. Cosmochim. Acta* **51**, 607–622.

WEBER D. AND BISCHOFF A. (1997) Refractory inclusions in the CR chondrite Acfer 059–El Djouf 001: Petrology, chemical composition, and relationship to inclusion populations in other types of carbonaceous chondrites. *Chem. Erde* **57**, 1–24.

WEISBERG M. K., PRINZ M., CLAYTON R. N., MAYEDA T. K., GRADY M. M. AND PILLINGER C. T. (1995) The CR chondrite clan. *Proc. NIPR Symp. Antarctic Meteorites* **8**, 11–32.

WOOD J. A. (1996) Unresolved issues in the formation of chondrules and chondrites. In *Chondrules and the Protoplanetary Disk* (eds. R. H. Hewins, R. H. Jones and E. R. D. Scott), pp. 55–71. Cambridge Univ. Press, Cambridge, U.K.

WOOD J. A. (1998a) Constraints placed by aluminum-26 on early solar system history (abstract). *Meteorit. Planet. Sci.* **33 (Suppl.)**, A168–A169.

WOOD J. A. (1998b) Meteoritic evidence for the infall of large interstellar dust aggregates during the formation of the solar system. *Astrophys. J.* **503**, L101–L104.

YURIMOTO H., KOIKE O., NAGAHARA H., MORIOKA M. AND NAGASAWA H. (2000) Heterogeneous distribution of Mg isotopes in anorthite single crystal from Type B CAI in Allende meteorite (abstract). *Lunar Planet. Sci.* **31**, #1593, Lunar and Planetary Institute, Houston, Texas, USA (CD-ROM).